# OPTIMIZATION OF SUPERSONIC ENGINE NOZZLE AT VARIOUS DIVERGENT ANGLES USING CFD

## A PROJECT REPORT

*Submitted by*

**MOGHAL RAHEL BAIG (U18AM026)**

*in partial fulfilment for the award of the degree of*

**BACHELOR OF TECHNOLOGY**

**in**

**AUTOMOBILE ENGINEERING**

**DEPARTMENT OF AUTOMOBILE ENGINEERING**

**BHARATH INSTITUTE OF HIGHER EDUCATION AND RESEARCH**

**CHENNAI – 600073**

**MAY 2022**

**BHARATH INSTITUTE OF HIGHER EDUCATION AND RESEARCH**

**CHENNAI – 600073**

# BONAFIDE CERTIFICATE

Certified that this project report "**OPTIMIZATION OF SUPERSONIC ENGINE NOZZLE AT VARIOUS DIVERGENT ANGLES USING CFD"** is the bonafide work of **MOGHAL RAHEL BAIG (U18AM026)** who carried out the project work under my supervision.


**Dr. D. RAGURAMAN**

**HEAD OF THE DEPARTMENT**

Associate Professor

Department of Automobile Engineering

BIHER

Selaiyur, Chennai – 73

**Mr. S. MANAVALAN**

**SUPERVISOR**

Assistant Professor

Department of Automobile Engineering

BIHER

Selaiyur, Chennai - 73


Submitted for the project viva-voce examination held on ……..

**INTERNAL EXAMINER** **EXTERNAL EXAMINER**

# ACKNOWLEDGEMENT

Before proceeding with the details of our project work we thank almighty god for making our endeavour as a successful one. From a twinkle of idea to visible reality this project has undergone many transitions and owes its success to enormous sources and many distinguished personalities.

I owe my sincere thanks and gratitude to my guide **Mr. S. MANAVALAN** for his incessant guidance and supervision in the project. Iam so grateful to thank him for his ideas and inspirations that encouraged me to proceed with the project.

I vogue debt of gratitude to **Dr. D. RAGURAMAN**, Head of the Department who have been helping me in ways both intellectual and emotional; his quick sacrifice of busy involvement in academic affairs is remarkable and I am always adore its trait.

I record my immense pleasure in whole heartedly expressing my sincere thanks to **Dr. J. HAMEED HUSSAIN**, Dean Engineering for providing the complete facilities to carry out this project.

I express my gratitude to our beloved Pro Vice-Chancellor (Academics)**Dr. M. SUNDARAJAN** in providing a valuable guidance and academic support towards the completion of the project.

I would like to place on records my heartfelt thanks to each and every faculty members of Department of Automobile Engineering for their inspirational guidance and my friends for their kind co-operation.

## ABSTRACT

CFD is a branch of Fluid Mechanics which rely on numerical methods and algorithms to solve and analyze problem that involves fluid flow. CFD analysis has been conducted to analyze flow pattern of supersonic rocket nozzle at various degree of divergent angle by using two dimensional axis-symmetric models, which solves governing equation by a control volume method. Variation in parameters like velocity, static pressure, turbulence intensity and temperature are being analyzed. Objective of this research is to investigate best suited divergent angle. The phenomena of oblique shock are visualized and it was found that at which degree of divergent angle it is completely eliminated from nozzle. Also intensity of velocity is found to have an increasing trend with increment in divergent angle thereby obtaining an optimum divergent angle which would eliminates instabilities due to shock and satisfies the thrust requirement from the nozzle.

# TABLE OF CONTENTS

# LIST OF FIGURES

## LIST OF FIGURES

# LIST OF TABLES

# CHAPTER 1

# INTRODUCTION

## 1.1 NOZZLE

A Nozzle (from nose, meaning 'small spout') is a tube of varying cross-sectional area (usually axi-symmetric) aiming at increasing the speed of an outflow, and controlling its direction and shape. Nozzle flow always generates forces associated to the change in flow momentum, as we can feel by handholding a hose and opening the tap. In the simplest case of a rocket nozzle, relative motion is created by ejecting mass from a chamber backwards through the nozzle, with the reaction forces acting mainly on the opposite chamber wall, with a small contribution from nozzle walls. As important as the propeller is to shaft-engine propulsions, so it is the nozzle to jet propulsion, since it is in the nozzle that thermal energy (or any other kind of high-pressure energy source) transforms into kinetic energy of the exhaust, and its associated linear momentum producing thrust.

The flow in a nozzle is very rapid (and thus adiabatic to a first approximation), and with very little frictional loses (because the flow is nearly one-dimensional, with a favourable pressure gradient except if shock waves form, and nozzles are relatively short), so that the isentropic model all along the nozzle is good enough for preliminary design. The nozzle is said to begin where the chamber diameter begins to decrease (by the way, we assume the nozzle is axisymmetric, i.e. with circular cross-sections, in spite that rectangular cross-sections, said two-dimensional nozzles, are sometimes used, particularly for their ease of directionability). The meridian nozzle shape is irrelevant with the 1D isentropic models; the flow is only dependent on cross-section area ratios.

Real nozzle flow departs from ideal (isentropic) flow on two aspects:

- Non-adiabatic effects. There is a kind of heat addition by non-equilibrium radical-species recombination and a heat removal by cooling the walls to keep the strength of materials in long duration rockets (e.g. operating temperature of cryogenic SR-25 rockets used in Space Shuttle is 3250 K, above steel vaporization temperature of 3100 K, not just melting, at 1700 K). Short duration rockets (e.g. solid rockets) are not actively cooled but rely on ablation; however, the nozzle-throat diameter cannot

let widen too much, and reinforced materials (e.g. carbon, silica) are used in the throat region.

- There is viscous dissipation within the boundary layer, and erosion of the walls, what can be critical if the erosion widens the throat cross-section, greatly reducing exit-area ratio and consequently thrust.
- Axial exit speed is lower than calculated with the one-dimensional exit speed, when radial outflow is accounted for. We do not consider too small nozzles, say with chamber size<10mm and neck size <1mm, where the effect of boundary layers become predominant. Restricting the analysis to isentropic flows, the minimum set of input parameters to define the propulsive properties of a nozzle (the thrust is the mass-flow-rate times the exit speed, F= mve) are
- Nozzle size, given by the exit area, Ae; the actual area law, provided the entry area is large enough that the entry speed can be neglected, only modifies the flow inside the nozzle, but not the exit conditions.
- Type of gas, defined with two independent properties for a perfect-gas model, that we take as the thermal capacity ratio $\gamma \equiv c_p/c_v$, and the gas constant, $R \equiv R_u/M$, and with $R_u$=8.314 J/(mol·K) and M being the molar mass, which we avoid using, to reserve the symbol M for the Mach number. If cp is given instead of γ, then we compute it from $\gamma \equiv c_p/c_v = c_p/(c_p - R)$, having used Mayer's relation, $c_p - c_v = R$.
- Chamber (or entry) conditions: pc and Tc (a relatively large chamber cross-section, and negligible speed, is assumed at the nozzle entry: $A_c \to \infty$, $M_c \to 0$). Instead of subscript 'c' for chamber conditions, we will use 't' for total values because the energy conservation implies that total temperature is invariant along the nozzle flow, and the non-dissipative assumption implies that total pressure is also invariant, i.e. Tt=Tc and pt=pc.
- Discharge conditions: p0, i.e. the environmental pressure (or back pressure), is the only variable of importance (because pressure waves propagate at the local speed of sound and quickly tend to force mechanical equilibrium.

The objective is to find the flow conditions at the exit [pe,Te,ve] for a given set of the above parameters, [Ae,γ ,R ,pc,Tc,,p0], so that:

$$\dot{m} = \rho_e v_e A_e = \frac{p_e}{R T_e} v_e A_e, \quad F = \dot{m} v_e, \quad M_e = \frac{v_e}{\sqrt{\gamma R T_e}}$$

Converging nozzles are used to accelerate the fluid in subsonic gas streams (and in liquid jets), since at low speeds density do not vary too much m= vA ρ const can be approximated by vA=const. Liquid&, and jets and low speed gas flows can be studied with classical Bernoulli equation (until cavitation effects appear in liquid flows), but high-speed gas dynamics is dominated by compressibility effects in the liquid. By the way, we do not considered here multiphase flow in nozzles. But when the flow is supersonic at some stage (even just at the exit), pe≠p0, and a more detailed analysis is required. Before developing it, let summarise the results

A converging nozzle can only become supersonic at the exit stage; the speed increases monotonically along the nozzle. If a converging nozzle is fed from a constant pressure constant temperature chamber, the flow rate grows as the discharge pressure is being reduced, until the flow becomes sonic (choked) and the flow rate no longer changes with further decreasing in discharge-pressure (a set of expansion waves adjust the exit pressure to this lower discharge pressure). Except for old-time turbojets and military fighter aircraft, all commercial jet engines (after Concorde was retired) use converging nozzles discharging at subsonic speed (both, the hot core stream and the colder fan stream).

A converging-diverging nozzle ('condi' nozzle, or CD-nozzle), is the only one to get supersonic flows with M>1 (when chocked). It was developed by Swedish inventor Gustaf de Laval in 1888 for use on a steam turbine. Supersonic flow in CD-nozzles presents a rich behaviour, with shock waves and expansion waves usually taking place inside and/or outside. Several nozzle geometries have been used in propulsion systems:

1. The classical quasi-one-dimensional Laval nozzle, which has a slender geometry, with a rapidly converging short entrance, a rounded throat, and a long conical exhaust of some 15º half-cone angle (the loss of thrust due to jet divergence is about 1.7%). Rarely used in modern rockets.
2. Bell-shape nozzles (or parabolic nozzles), which are as efficiency as the simplest conical nozzle, but shorter and lighter, though more expensive to manufacture. They are the present standard in rockets; e.g. the Shuttle main engine (SME) nozzles yield 99% of the ideal nozzle thrust (and the remainder is because of wall friction, not because of wall shape effect).
3. Annular and linear nozzles, designed to compensate ambient pressure variation, like the Aerospike nozzle. They are under development.

4. We present below the 1D model of gas flow in nozzles. For more realistic design, beyond this simple model, a 2D (or axisymmetric) analysis by the method of characteristics and boundary layer effects should follow, to be completed with a full 3D nozzle-flow analysis by CFD.

## 1.2 NOZZLE FLOW EQUATIONS

Let us consider the steady isentropic 1D gas dynamics in a CD-nozzle, with the perfect gas model (i.e. pV=mRT and, taking T=0 K as energy reference, h=cpT). Conservation of mass, momentum, and energy, in terms of the Mach number, M≡ v/c (where c = γRT stands for the sound speed), become:

$$\dot{m} = \rho v A = \text{const} = \frac{p}{RT}\left(M\sqrt{\gamma RT}\right)A \quad \rightarrow \quad \frac{\mathrm{d}p}{p} - \frac{\mathrm{d}T}{2T} + \frac{\mathrm{d}M}{M} + \frac{\mathrm{d}A}{A} = 0$$

$$\rho v \mathrm{d}v = -\mathrm{d}p \rightarrow \frac{\mathrm{d}v^2}{2} + \frac{\mathrm{d}p}{\rho} = 0 \xrightarrow{dh=Tds+vdp} \frac{\mathrm{d}v^2}{2} + \mathrm{d}h - T\mathrm{d}s = 0 \xrightarrow{h_t=h+\frac{v^2}{2}=\text{const}} \mathrm{d}s = 0$$

$$h_t = h + \frac{v^2}{2} = \text{const} = c_p T + \frac{1}{2}M^2\gamma RT \quad \rightarrow \quad \frac{\mathrm{d}T}{T}\left(1 + \frac{\gamma-1}{2}M^2\right) + (\gamma-1)M\mathrm{d}M = 0$$

where logarithmic differentiation has been performed. Notice that, with this model, the isentropic condition can replace the momentum equation, so that differentiation of the isentropic relations for a perfect gas T/p(γ−1)/γ=const, yields:

$$\frac{\mathrm{d}T}{T} = \frac{\gamma-1}{\gamma}\frac{\mathrm{d}p}{p}$$

The energy balance (Δht=q+w) implies the conservation of total enthalpy and total temperature (ht=cpTt), and the non-friction assumption implies the conservation of total pressure (pt), with the relations between total and static values given by:

$$\frac{T_t}{T} = 1 + \frac{v^2}{2c_p T} = 1 + \frac{\gamma-1}{2}M^2 = \left(\frac{p_t}{p}\right)^{\frac{\gamma-1}{\gamma}}$$

Notice that, with the perfect gas model, γ remains constant throughout the expansion process. However, when the engine flow is composed of hot combustion products, real gas effects become important, and as the gas expands, γ shifts as a result of changes in temperature and in chemical composition. Maximum thrust is obtained if the gas

composition is in chemical equilibrium throughout the entire nozzle expansion process.Choosing the cross-section area of the duct, A, as independent variable, the variation of the other variables can be explicitly found to be:

$$\left(1-M^2\right)\frac{\mathrm{d}T}{T}=(\gamma-1)M^2\frac{\mathrm{d}A}{A} \tag{8}$$

$$\left(1-M^2\right)\frac{\mathrm{d}p}{p}=\gamma M^2\frac{\mathrm{d}A}{A} \tag{9}$$

$$\left(1-M^2\right)\frac{\mathrm{d}M}{M}=-\left(1+\frac{\gamma-1}{2}M^2\right)\frac{\mathrm{d}A}{A} \tag{10}$$

$$\left(1-M^2\right)\frac{\mathrm{d}v}{v}=-\frac{\mathrm{d}A}{A} \tag{11}$$

**1.3 TYPES OF NOZZLE:**

**CONVERGING NOZZLE**

In a converging nozzle, cross-section area smoothly decreases from a larger value (usually assumed a plenum chamber with M→0, pc=pt) to a smaller value (exit section Ae, with Me and pe). The mass flow rate in terms of static or total conditions at any stage, with the isentropic relations (7), is:

$$\dot{m}=\rho vA=\sqrt{\frac{\gamma}{R}}\frac{p}{\sqrt{T}}MA=\sqrt{\frac{\gamma}{R}}\frac{p_t}{\sqrt{T_t}}\left(1+\frac{\gamma-1}{2}M^2\right)^{-\frac{\gamma+1}{2(\gamma-1)}}MA$$

m=const,Tt=const,pt=const. Whatever the area law, the flow accelerates to a maximum speed at the&with m exit.

Two cases may appear:

- Subsonic exit (Me<1)
- Sonic exit (Me=1).

For subsonic exit, exit pressure equals ambient pressure (pe=p0), and exit conditions are:

$$p_e=p_0,\quad T_e=T_t\left(\frac{p_e}{p_t}\right)^{\frac{\gamma-1}{\gamma}},\quad M_e=\sqrt{\frac{2}{\gamma-1}\left(\left(\frac{p_t}{p_e}\right)^{\frac{\gamma-1}{\gamma}}-1\right)},\quad \dot{m}=\sqrt{\frac{\gamma}{R}}\frac{p_t}{\sqrt{T_t}}\left(1+\frac{\gamma-1}{2}M_e^2\right)^{-\frac{\gamma+1}{2(\gamma-1)}}M_eA_e$$

valid only if Me≤1. The limit Me=1 (choking conditions) will be reached when:

$$\frac{p_e}{p_t}=\left(\frac{2}{\gamma+1}\right)^{\frac{\gamma}{\gamma-1}},\quad \frac{T_e}{T_t}=\frac{2}{\gamma+1},\quad M_e=1,\quad \dot{m}=\sqrt{\frac{\gamma}{R}}\frac{p_t}{\sqrt{T_t}}\left(\frac{\gamma+1}{2}\right)^{-\frac{\gamma+1}{2(\gamma-1)}}A_e=\frac{\gamma p_t}{c_c}\left(\frac{\gamma+1}{2}\right)^{-\frac{\gamma+1}{2(\gamma-1)}}A_e$$

where $c_c=\sqrt{\gamma RT_t}$ is the sound speed at chamber conditions. In conclusion, if, for given entry conditions (pt and Tt), ambient pressure is being lowered from the no-flow condition, p0=pt, first a subsonic flow develops, until p0=p* =pt(2/(γ+1))γ/(γ−1), e.g. p0/pt=0.53 for γ=1.4, where mass flow rate is at a maximum, and a further decrease of ambient pressure has no effect in nozzle flow (no pressure-information can go upstream); a fan of oblique supersonic expansion waves appears just at the exit, to accommodate exit pressure pe to ambient pressure p0<pe with a bulging of the exhaust jet.

The flow will separate at the maximum constriction (the throat), and will behave as a converging nozzle. If the feeding chamber is at a steady state (i.e. Tt=const, pt=const), then the choked flow is invariant, and the mass-flow-rate a constant, (17), for given exit area Ae, no matter how much the discharge pressure is lowered. But, if the feeding chamber is unsteady, e.g. depressurising because of the escaping mass, then, even if the nozzle remains choked, the mass flow rate, given by, decreases with time, with the following invariant:

$$\frac{\dot{m}\sqrt{T_t}}{p_t}=\text{const}$$

i.e m changes with changing entry conditions. The two extreme cases of discharge from a gas tank are isothermal (Tt=const, so that m ∝ pc), and adiabatic (isentropic, if internal dissipation is negligible, i.e Tt=const·pt (γ−1)/γ ,Notice that a gas tank discharges more slowly if thermally isolated than if kept isothermal (in the latter, heat addition tends to increase pressure and help the ejection).

**CONVERGING-DIVERGING NOZZLE**

A converging-diverging nozzle ('condi' nozzle, or CD-nozzle) must have a smooth area law, with a smooth throat, dA/dx=0, for the flow to remain attached to the walls. The flow starts from rest and accelerates subsonically to a maximum speed at the throat, where it may arrive at M<1 or M=1 as for converging nozzles. Again, for the entry conditions we

use 'c' (for chamber) or't' (for total), we use 'e' for the exit conditions, and '*' for the throat conditions when it is choked (M* =1).

If the flow is subsonic at the throat, it is subsonic all along the nozzle, and exit pressure pe naturally adapts to environmental pressure p0 because pressure-waves travel upstream faster (at the speed of sound) than the flow (subsonic), so that pe/p0=1. But now the minimum exit pressure for subsonic flow is no longer pe=pt(2/(γ+1))γ/(γ−1) (pe/p0=0.53 for γ=1.4), since the choking does not take place at the exit but at the throat, i.e. it is the throat condition that remains valid, p* =pt(2/(γ+1))γ/(γ−1), e.g. p* /p0=0.53 for γ=1.4; now the limit for subsonic flow is pe,min,sub>p* because of the pressure recovery in the diverging part. However, if the flow is isentropic all along the nozzle, be it fully subsonic or supersonic from the throat, the isentropic equations apply

$$\left(\frac{p_t}{p_e}\right)^{\frac{\gamma-1}{\gamma}} = \frac{T_t}{T_e} = 1+\frac{\gamma-1}{2}M_e^2, \quad M_e = \sqrt{\frac{2}{\gamma-1}\left(\left(\frac{p_t}{p_e}\right)^{\frac{\gamma-1}{\gamma}}-1\right)}$$

$$\dot{m} = \rho_e v_e A_e = \frac{\gamma p_t A_e}{\sqrt{\gamma R T_t}} M_e \left(1+\frac{\gamma-1}{2}M_e^2\right)^{\frac{2-\gamma}{2}}$$

But if the flow gets sonic at the throat, several downstream conditions may appear. The control parameter is discharge pressure, p0. Let consider a fix-geometry CD-nozzle, discharging a given gas from a reservoir with constant conditions (pt,Tt). When lowering the environmental pressure, p0, from the no flow conditions, p0=pt, we may have the following flow regimes (a plot of pressure variation along the nozzle is sketched in Fig

- Subsonic throat, implying subsonic flow all along to the exit.
- Sonic throat (no further increase in mass-flow-rate whatever low the discharge pressure let be).
    - Fully subsonic flow except at the throat (evolution b).
    - Flow becomes supersonic after the throat, but, before exit, a normal shockwave causes a sudden transition to subsonic flow (evolution c). It may happen that the flow detaches from the wall (see the corresponding sketch).
- ❖ Flow becomes supersonic after the throat, with the normal shockwave just at the exit section (evolution d).

- Flow becomes supersonic after the throat, and remains supersonic until de exit, but there, three cases may be distinguished
  - Oblique shock-waves appear at the exit, to compress the exhaust to the higher back pressure (evolution e). The types of flow with shock-waves (c, d and e in Fig.) are named 'over-expanded' because the supersonic flow in the diverging part of the nozzle has lowered pressure so much that a recompression is required to match the discharge pressure. That is the normal situation for a nozzle working at low altitudes (assuming it is adapted at higher altitudes); it also occurs at short times after ignition, when chamber pressure is not high enough.
  - Adapted nozzle, where exit pressure equals discharge pressure (evolution f). Notice that, as exit pressure pe only depends on chamber conditions for a choked nozzle, a fix-geometry nozzle can only work adapted at a certain altitude (such that p0(z)=pe).
  - Expansion waves appear at the exit, to expand the exhaust to the lower back pressure (evolution e); this is the normal situation for nozzles working under vacuum. This type of flow is named 'under-expanded' because exit pressure is not low-enough, and additional expansion takes place after exhaust.

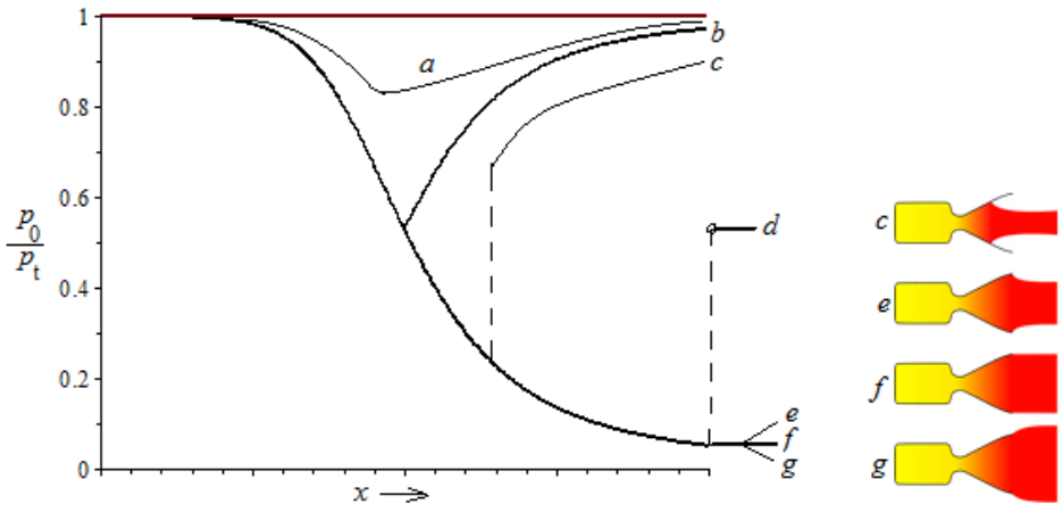


**Fig1.1: Nozzle flows for constant entry conditions (pt,Tt)**

As a function of discharge pressure p0. As p0 is being decreased, the flow starts being subsonic (a) all along the nozzle length (x), then it becomes choked (and the flow no longer changes in the converging part). But the flow in the diverging part may be subsonic (b), or a transition from supersonic to subsonic occur within (c, from b to d), or the supersonic flow at the exit be followed by compression waves (e), be adapted (f), or be

followed by expansion waves (g); the latter case is said under-expanded, and is typical under vacuum.

In the converging-diverging nozzle used in supersonic aircraft, both the throat area and the exit area should be optimised for maximum thrust as a function of altitude and flight speed, but in practice there is a single mechanical adjustment, using petals to achieve a variable area nozzle. In rockets, a fix-area nozzle is the rule. When the flow is isentropic all along the nozzle, i.e. for values of p0/pt from d to g in the exit Mach number Me is given by:

$$\frac{A^*}{A_e} = M_e \left( \frac{\frac{\gamma+1}{2}}{1+\frac{\gamma-1}{2}M_e^2} \right)^{\frac{\gamma+1}{2(\gamma-1)}}$$

Mind that, solving for M yields two solutions,

$$\left( \frac{p_t}{p_{e,sub}} \right)^{\frac{\gamma-1}{\gamma}} = \frac{T_t}{T_{e,sub}} = 1+\frac{\gamma-1}{2}M_{e,sub}^2$$

$$\left( \frac{p_t}{p_{e,sup}} \right)^{\frac{\gamma-1}{\gamma}} = \frac{T_t}{T_{e,sup}} = 1+\frac{\gamma-1}{2}M_{e,sup}^2$$

The supersonic mass-flow-rate and exit speed in the isentropic discharge through a nozzle are:

$$\dot{m} = \rho^* v^* A^* = \frac{p^*}{RT^*}\sqrt{\gamma RT^*}\,A^* = \frac{\gamma p^* A^*}{\sqrt{\gamma RT^*}} = \frac{\gamma p_t A^*}{\sqrt{\gamma RT_t}}\left(\frac{2}{\gamma+1}\right)^{\frac{\gamma+1}{2(\gamma-1)}}$$

$$v_e = \sqrt{\frac{2\gamma RT_t}{\gamma-1}\left[1-\left(\frac{p_e}{p_t}\right)^{\frac{\gamma-1}{\gamma}}\right]} = \sqrt{\frac{2\gamma RT_t}{\gamma-1}\left[1-\frac{1}{1+\frac{\gamma-1}{2}M_e^2}\right]}$$

Notice that, although it is often said that m meant is that the mass-flow-rate does not depend on back pressure (provided the flow becomes  is almost proportional to chamber pressure (and depends on temperature and gas&supersonic), but m properties too; though

they are almost invariable during normal operation of rockets; see Chamber pressure equation, below.

Sometimes, a characteristic speed vc is defined as chamber pressure (pt) times throat area (A* ) divided by ), i.e. by *&mass flow rate ( m , a modified sound speed independent of the exit area, as can be&c t v pA m ≡ deduced by substitution from (23); when using such a characteristic speed, a non-dimensional thrust coefficient is defined by cF≡F/(ptA* )=ve/vc+(Ae/A* )(pe−p0)/pt, such that for an adapted nozzle it is cF=ve/vc.

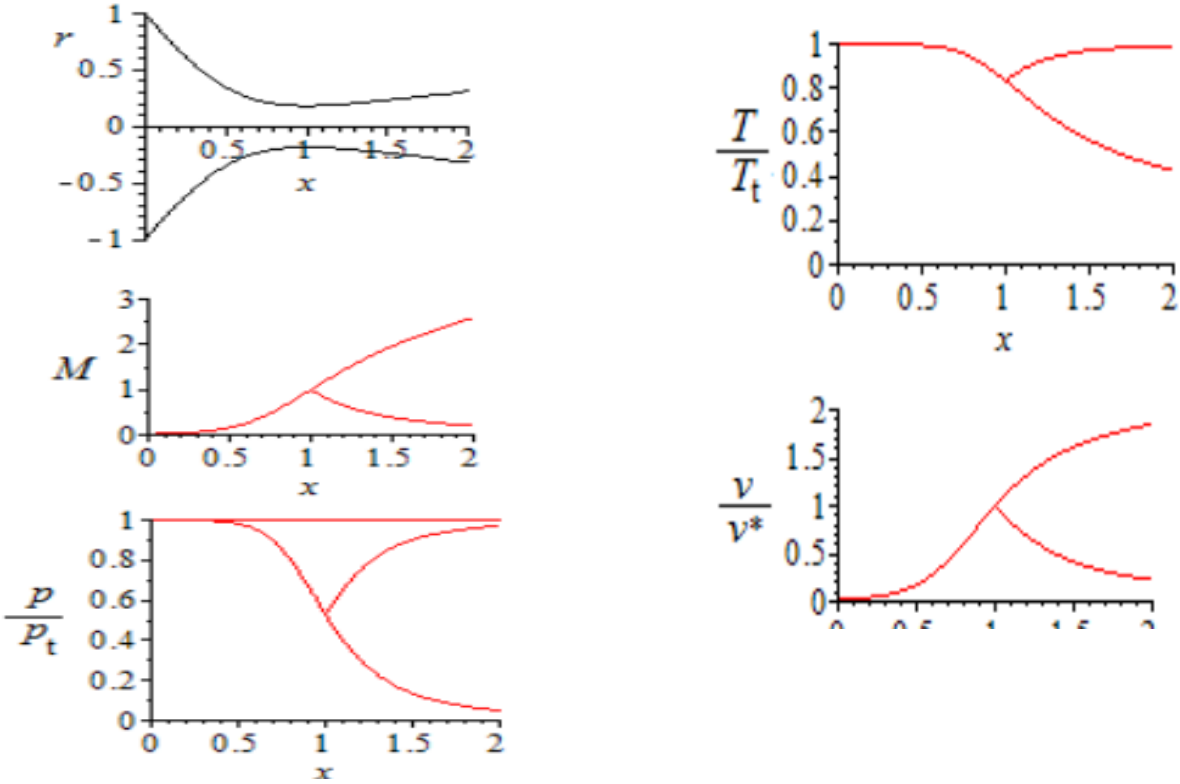


**Fig 1.2: CD-nozzle flow**

Fig. A computed example of choked flow of air (γ=1.4) in the CD-nozzle geometry shown on top (nozzle throat at x=1; in scaled arbitrary dimensions, area ratio Ae/A* =2.9). Two isentropic solutions exist: one totally subsonic (except at the throat, which is sonic), and another that becomes supersonic after the throat. The plots are: Mach number, local pressure relative to chamber value, local temperature relative to chamber value, and local speed relative to its throat value (speed of sound at throat conditions). More detailed nozzle flow simulations can be found aside.

Looking at the smooth rounding of the nozzle neck (Fig. 3a), it seems amazing the kink in all flow variables corresponding to the full subsonic solution (the explanation

resides in the singularity that (8) - (11) have for M=1). Another astonishing result is the very rapid pressure changes at the neck: in the length from x=0.86 to x=1.18 in Fig. 3a, where the nozzle radius varies from r=0.19 to r=0.19 through r=0.18 at the throat (a 10 % in area change from neck to ends), pressure (scaled with the constant total pressure) varies from p/pt=0.73 at x=0.86 to p/pt=0.32 at x=1.18 if the flow becomes supersonic (or recedes to the same subsonic value, p/pt=0.73 at x=1.18 if it remains subsonic), passing by p* /pt=0.53 at x=1; i.e. between the two sections with radius 5 % larger than the minimum, pressure decreases a 56% (in supersonic flow; or it recovers, after decreasing a 27%). It is also impressive how soon the choking occurs when backpressure pe is being decreased: at pe/pt=1 there is no flow, and at pe/pt=0.97 the nozzle is already choked, with a fix mass flow rate whatever the value of pe/pt<.97 (if entry conditions are maintained). But, if the flow is choked, how it adapts to the changing exit pressure? Through discontinuities in the flow, breaking the isentropic condition.

## 1.4 DISCONTINUITIES IN NOZZLE FLOW

## NORMAL AND OBLIQUE SHOCKS, EXPANSION FANS. MACH DIAMONDS

Consider the isentropic pressure evolution along the nozzle in Fig. 2, Far downstream of the exit stage, the exhaust jet (say, more than a couple of exit diameters), the jet , leaving aside a possible adjustment close to the exit, must be sensibly equal the exit pressure

We have seen that, for given entry conditions, several cases of nozzle flow appear as a function of the imposed discharge pressure p0, to which the exhaust jet must adapt, since a free jet cannot withstand transversal pressure gradients. This pressure-adaptation may be through small (linear) or strong (nonlinear) pressure waves. By comparing relative exit pressure pe/pt, with relative back pressure p0/pt, the possible flow configurations are:

- If 1>pe/pt>pe,sub/pt, then the matching pe=p0 is by acoustic waves travelling upstream from the exit to the entrance, and the flow is subsonic all along the nozzle length; for the example plotted in Fig., 1>pe/pt>0.97.
- If pe/pt=pe,sub/pt, the flow is choked but subsonic except at the neck (this is the limit of the case above).

- If pe,sub/pt>pe/pt>pe,sup/pt, then the matching pe=p0 is by acoustic waves travelling upstream from the exit to a section between exit and throat, where a strong shock takes place; the location of this normal shockwave develops some distance downstream (the further down the lower the backpressure), with subsonic flow beyond, matching the ambient backpressure. For the example plotted in Fig. 3, this range is 0.97>pe/pt>0.05. This nozzle-flow configuration is known as overexpanded (see Fig. 2).
    - The shockwave is inside the nozzle if pe,sub/pt>pe/pt>pe,es/pt, where pe,es is the exit pressure with exit shock wave; for the example plotted in Fig. 3, 0.97>pe/pt>0.39. The value of pe,es is found by using the normal-shockwave pressure-jump equation with pe,sup and Me,sup as upstream conditions. The sudden compression at the normal shock, and the subsequentunfavourable pressure-gradient, makes this subsonic flow to detach from the wall, what is often termed 'grossly over-expanded flow', what yields poor nozzle performances (the typical behaviour on ground of nozzles designed for high-altitude and vacuum operation).

**NORMAL SHOCK WITHIN NOZZLE**

A normal shock generates entropy and thus lowers total pressure (while greatly increasing static pressure). Mass flow-rate conservation relates both values: total pressure before, *p*t, and after the shock, *p*te (exit total pressure). Applying (15) to throat and exit conditions (at each side of the shock):

$$\dot{m} = \sqrt{\frac{\gamma}{R}} \frac{p_t}{\sqrt{T_t}} \left(1+\frac{\gamma-1}{2}\right)^{1-\frac{\gamma}{2}} A^* = \sqrt{\frac{\gamma}{R}} \frac{p_{te}}{\sqrt{T_t}} \left(1+\frac{\gamma-1}{2} M_e^2\right)^{1-\frac{\gamma}{2}} M_e A$$

now we get, instead of (14):

$$\frac{p_t A^*}{p_{te} A_e} = \frac{1}{M_e} \left( \frac{\frac{\gamma+1}{2}}{1+\frac{\gamma-1}{2} M_e^2} \right)^{\frac{\gamma+1}{2(\gamma-1)}} , \quad \text{with } p_{te} = p_0 \left(1+\frac{\gamma-1}{2} M_e^2\right)^{\frac{\gamma}{\gamma-1}}$$

where we have to solve for *M*e for given entry and exit pressure (*p*t, *p*0), and throat and exit area (*A**,*A*e).Once the total pressure loss computed, the actual Mach number just before the shock wave, *M*s, is found from
normal-shock relations:

$$\frac{p_{te}}{p_t} = \left( \frac{\frac{\gamma+1}{2} M_s^2}{1 + \frac{\gamma-1}{2} M_s^2} \right)^{\frac{\gamma}{\gamma-1}} \left( \frac{\frac{\gamma+1}{2}}{\gamma M_s^2 - \frac{\gamma-1}{2}} \right)^{\frac{1}{\gamma-1}}$$

Solving for this shock-entry Mach number, *M*s, allows the spatial location of the front within the nozzle interms of areas, from (20). In particular, the shock wave is located precisely at the exit section when thejump in Mach number across yields a downstream pressure, *p*e,es (impinging pressure is *p*e,sup), equal tothe environmental pressure, *p*0, i.e. when:

$$\frac{p_t}{p_0} = \frac{A_e}{A^*} \left( \frac{\gamma+1}{2} \right)^{\frac{\gamma+1}{2(\gamma-1)}} M_2 \sqrt{1 + \frac{\gamma-1}{2} M_2^2}, \quad \text{with } M_2 = \sqrt{\frac{1 + \frac{\gamma-1}{2} M_1^2}{\gamma M_1^2 - \frac{\gamma-1}{2}}}$$

where *M*1 and *M*2 are the Mach numbers ahead and behind the normal shock wave (*M*1=*M*s). The specificentropy generation in the normal chock is *s*gen=*s*2−*s*1=*cp*ln(*T*2/*T*1)−Rln(*p*2/*p*1)=−*R*ln(*p*te/*p*t).

## OBLIQUE SHOCKS AT NOZZLE EXIT

Shock diamonds (or Mach diamonds) are patterns of standing waves that appears in the supersonic exhaust plume of aerospace propulsion system (turbojet with post-combustor, solid- or liquid-fuel rocket,ramjet, or scramjet), when operated in an atmosphere with *p*0>*p*e (i.e. when the flow is over-expanded in aCD-nozzle. When the exhaust flow gets across a normal shock (in red in Fig. 5a) the abrupt compression causes a sudden temperature increase, with radicals producing non-equilibrium chemiluminescence, which in the case of LH2/LOX rockets is composed of a weak emission-continuum in the blue and ultraviolet regions of the spectrum, and a 20 times stronger narrow-band emission at 310 nm, due to excitation of OH and H radicals and their recombination to H2O. Besides, this sudden heating may cause the ignition of any residual fuel present in the exhaust, making the Mach disc and trail to glow and become visible like in

Fig. Behind the normal shock, the pressure is greater than that of the ambient atmosphere, so that the jet expands, trying to equalize with the external air (the expanding waves reflect off the free jet boundary and towards the centerline), what may require several expansions and compressions. A similar process occurs in an under-expanded flow exiting from a nozzle at high altitude or under vacuum (Fig. 5b). The sequence of compression and expansion is identical to that above-described for an over-expanded nozzle, except that it begins with the creation of an expansion fan rather than oblique shock waves. This behavior causes the flow to billow outward initially rather than spindle inward.

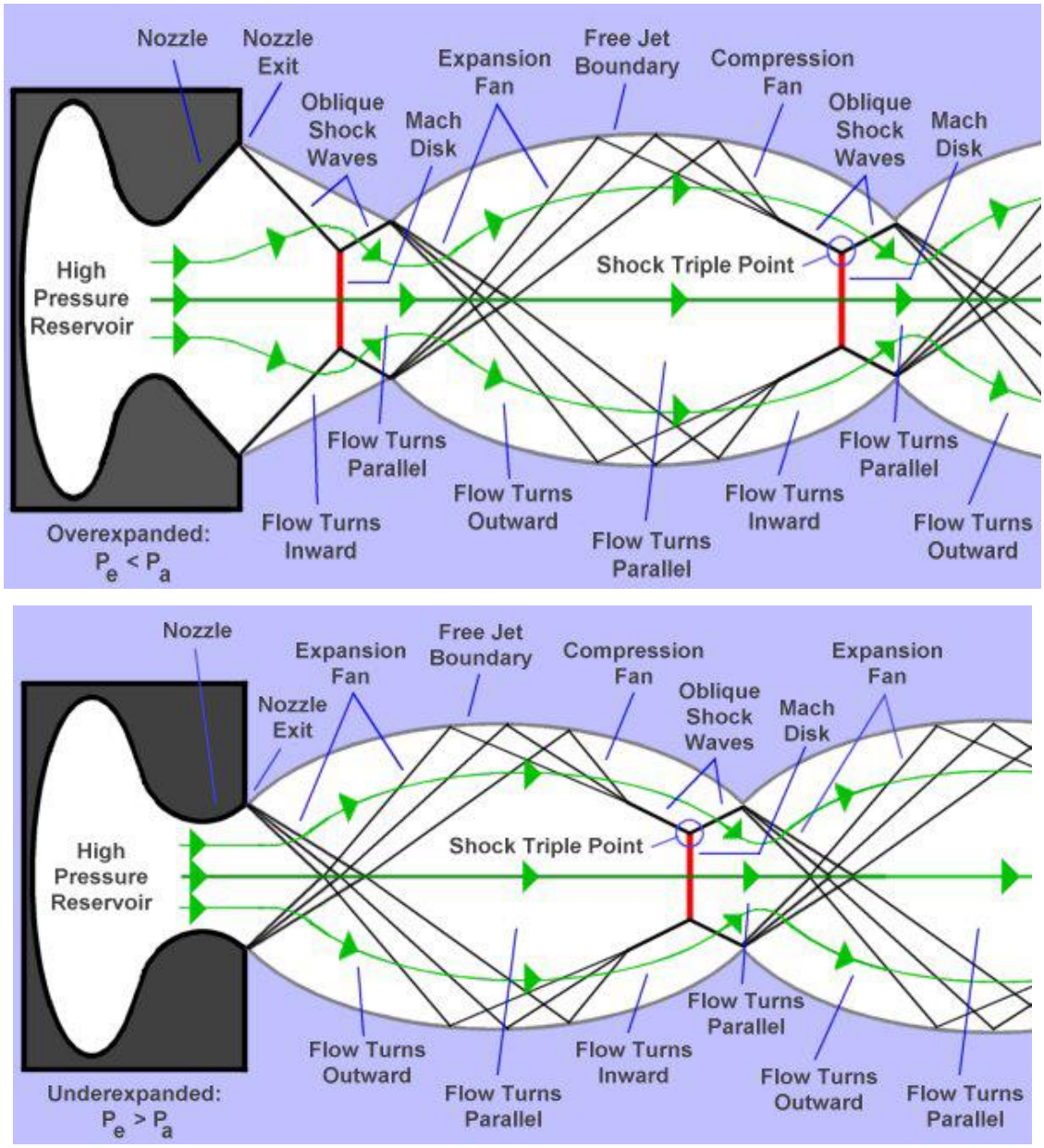


**Fig 1.3: Shock diamonds in an over-expanded flow**

The first Mach disc (in red) is separated from theexit by $x\ De = (2\ 3)\ p0\ pe$ . b) Wave structures that create shock diamonds in an underexpanded flow (Aerospaceweb).

## AEROSPIKE NOZZLE

This is a novel design for a fix-geometry nozzle to get adapted at all altitudes. Instead of an outward flow in a bell-shape wall boundary, in the aerospike nozzle an annular flow issues radially inward along a decreasing-diameter inner wall (the spike), without external wall (after a cowl lip), see Fig. 6. The outer ambient pressure regulates the outer plume boundary so that when $pe<p0$ (over-expansion at low altitudes)
the external pressure squeezes and makes the plume thinner, further accelerating the exhaust instead of detaching it from the walls. Since ambient pressure controls the nozzle expansion, the flow area at the end of the aerospike changes with altitude, as if it was a variable-area nozzle, and thus, a very high area ratio nozzle, which provides high vacuum performance, can also be efficiently operated at sea level. The length of an ideal spike is about 150 % of a 15° conical nozzle, but performances reduce very little if the spike length is truncated to the 20 % range, with the formation of a recirculating bubble which, if fed with a secondary jet at the base, elongates the bubble, forming an aerodynamic contour that resembles the truncated portion of the spike (this aerodynamic-shape is the reason for the "aerospike" term).

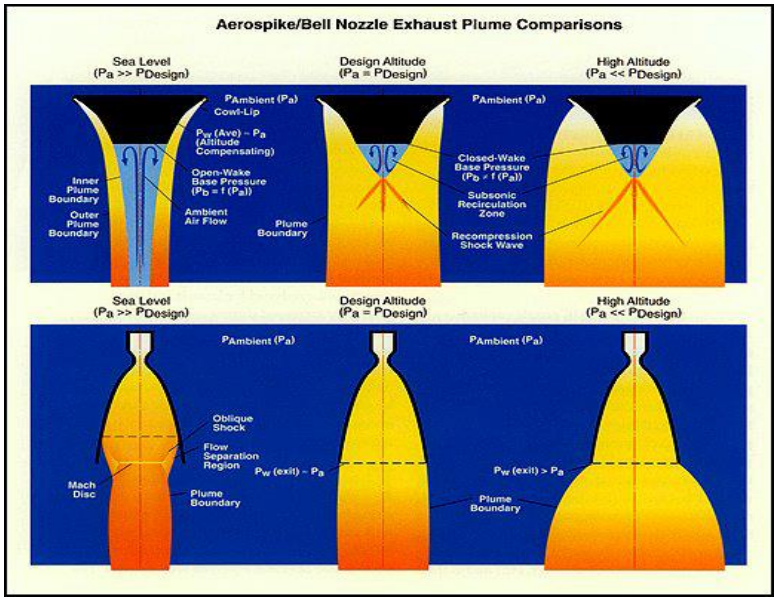


**Fig 1.4: Different flow configurations in aerospike nozzles and comparison with bell nozzles back to Propulsion**

## 1.5 INTRODUCTION TO CFD

Nowadays, Computational fluid dynamics (CFD) has become a progressively handy and robust tool for the numerical analysis involving transport processes. CFD provides understanding into flow design, which are laborious, costly or impossible to investigate using conventional techniques. It consists of simulation of multiphase flow, heat transfer, chemical reactions and particulate processes. In CFD simulations, accuracy and reliability are the main factors upon which emphasize is given. It is broadly accepted that simulations performed by CFD are very susceptible to the various computational parameters that have to be set by the user. Consequently, CFD verification and validation studies are crucial, as well as comprehensive sensitivity studies that can deliver effective guidance in the selection of computational variables for future CFD studies.

### CONCEPT OF COMPUTATIONAL FLUID DYNAMICS

Computational Fluid Dynamics (CFD) is the simulation of fluids engineering systems using modelling (mathematical physical problem formulation) and numerical methods (discretization methods, solvers, numerical parameters, and grid generations, etc.).

The process of Computational Fluid Dynamics firstly, we have a fluid problem. To solve this problem, we should know the physical properties of fluid by using Fluid Mechanics. Then we can use mathematical equations to describe these physical properties. This is Navier-Stokes Equation and it is the governing equation of CFD.

The governing equations for fluid flow can then be applied to each section individually, but as the properties of each section are inevitably linked to its neighbouring sections, all the sections can be solved simultaneously until a full solution for the entire flow field can be found. This method obviously requires a huge amount of computational power, nevertheless with the advancement of modern computing, solutions that would take months to compute by hand can now be found in seconds using nothing more than an ordinary desktop or laptop computer. Its accuracy or validity are dependent on a multitude of different factors: the quality and appropriateness of the mesh, the degree to which the chosen equations match the type of flow to be modelled, the interpretation of the results,

the accuracy of the boundary conditions entered by the user or the level of convergence of the solution, to name but a few.

The typical languages are FORTRAN and C. Normally the programs are run on workstations or supercomputers. At the end, we can get our simulation results. This below figure shows the process of CFD.

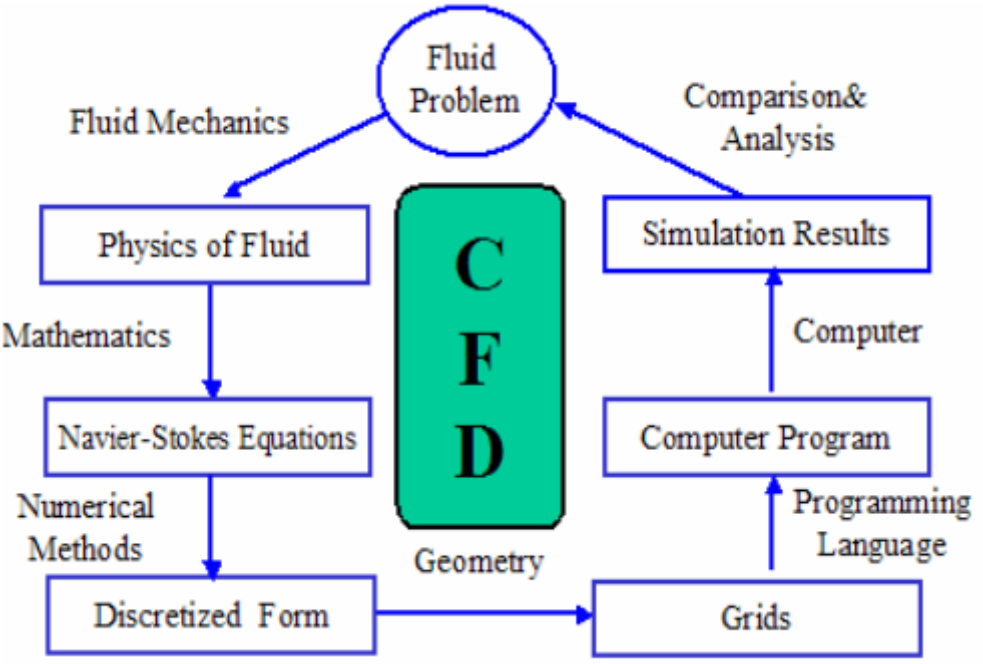


**Fig 1.5: Process of CFD**

**BACKGROUND AND HISTORY**

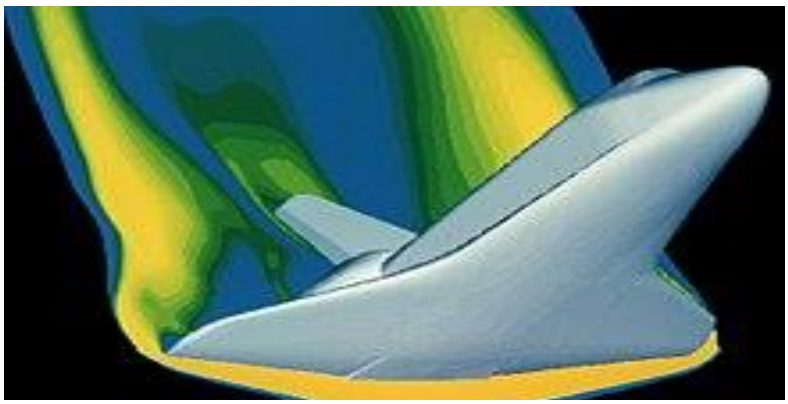

**Fig 1.6: A computer simulation of high velocity air flow around the Space Shuttle during re-entry**

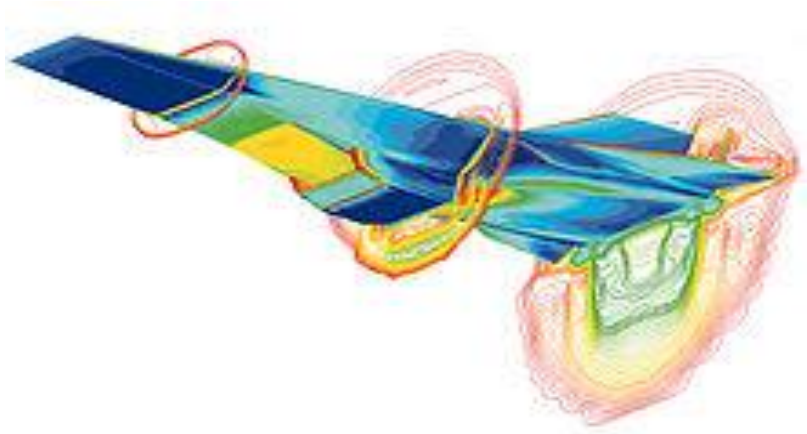

**Fig 1.7: A simulation of the Hyper-X scramjet vehicle in operation at Mach7**

The fundamental basis of almost all CFD problems is the Navier–Stokes equations, which define many single-phase (gas or liquid, but not both) fluid flows. These equations can be simplified by removing terms describing viscous actions to yield the Euler equations. Further simplification, by removing terms describing vorticity yields the full potential equations.

Finally, for small perturbations in subsonic and supersonic flows (not transonic or hypersonic) these equations can be linearized to yield the linearized potential equations. Historically, methods were first developed to solve the linearized potential equations. Two-dimensional (2D) methods, using conformal transformations of the flow about a cylinder to the flow about an air foil were developed in the 1930s.

One of the earliest types of calculations resembling modern CFD are those by Lewis Fry Richardson, in the sense that these calculations used finite differences and divided the physical space in cells. Although they failed dramatically, these calculations, together with Richardson's book "Weather prediction by numerical process", set the basis for modern CFD and numerical meteorology. In fact, early CFD calculations during the 1940s using ENIAC used methods close to those in Richardson's 1922 book.

The computer power available paced development of three-dimensional methods. Probably the first work using computers to model fluid flow, as governed by the Navier-Stokes equations, was performed at Los Alamos National Lab, in the T3 group. This group was led by Francis H. Harlow, who is widely considered as one of the pioneers of CFD.

From 1957 to late 1960s, this group developed a variety of numerical methods to simulate transient two-dimensional fluid flows, such as Particle-in-cell method (Harlow,1957), Fluid-in-cell method (Gentry, Martin and Daly, 1966), Vorticity stream function method (Jake Fromm, 1963), and Marker-and-cell method (Harlow and Welch, 1965). Fromm's vorticity-stream-function method for 2D, transient, incompressible flow was the first treatment of strongly contorting incompressible flows in the world.

The first paper with three-dimensional model was published by John Hess and A.M.O. Smith of Douglas Aircraft in 1967.Their method itself was simplified, in that it did not include lifting flows and hence was mainly applied to ship hulls and aircraft fuselages. The first lifting Panel Code (A230) was described in a paper written by Paul Rubbert and Gary Saaris of Boeing Aircraft in 1968. In time, more advanced three-dimensional Panel Codes were developed at,Boeing(PANAIR,A502), Lockheed (Quadpan),Douglas (HESS), McDonnell,Aircraft (MACAERO), NASA (PMARC) and Analytical Methods (WBAERO, USAERO and VSAERO). Some (PANAIR, HESS and MACAERO) were higher order codes, using higher order distributions of surface singularities, while others (Quadpan, PMARC, USAERO and VSAERO) used single singularities on each surface panel.

**What is CFD?**

Computational Fluid Dynamics (CFD) provides a qualitative (and sometimes even quantitative) prediction of fluid flows by means of

- mathematical modeling (partial differential equations)
- numerical methods (discretization and solution techniques)
- software tools (solvers, pre- and post-processing utilities)

**Why use CFD?**

Numerical simulations of fluid flow (will) enable

- Architects to design comfortable and safe living environments
- Designers of vehicles to improve the aerodynamic characteristics
- Chemical engineers to maximize the yield from their equipment
- Petroleum engineers to devise optimal oil recovery strategies
- Surgeons to cure arterial diseases (computational thermodynamics)

## Importance of Computational Fluid Dynamics

There are three methods in study of Fluid: theory analysis, experiment and simulation (CFD). As a new method, CFD has many advantages compared to experiments.

**Table 1.1 Comparisons of Simulation and Experiment**

| **Parameters** | **Simulation (CFD)** | **Experiment** |
|---|---|---|
| Cost | Cheap | Expensive |
| Time | Short | Long |
| Scale | Any | Small/Middle |
| Information | All | Measured Point |
| Repeatable | Yes | Some |
| Safety | Yes Some | Dangerous |

## Application of Computational Fluid Dynamics

As CFD has so many advantages, it is already generally used in industry such as aerospace, automotive, biomedicine, chemical processing, heat ventilation air condition, hydraulics, power generation, sports and marine etc.

## Boundary Conditions

To solve the equation system, we also need boundary conditions. The typical boundary conditions in CFD are No-slip boundary condition, Axisymmetric boundary condition, Inlet, outlet boundary condition and Periodic boundary condition.
The fluid flows from left to right. We can use inlet at left side, which means we can set the velocity manually.

At the right side, we use outlet boundary condition to keep all the properties constant, which means all the gradients are zero. At the wall of pipe, we can set the velocity to zero. This is no-slip boundary condition. At the center of pipe, we can use axisymmetric boundary condition.

## 1.6 POST PROCESSING

Post processing of the simulation results is performed in order to extract the desired information from the computed flow field

- Calculation of derived quantities (stream function, vorticity)
- Calculation of integral parameters (lift, drag, total mass)

1D data : function values connected by straight lines

2D data : streamlines, contour levels, colour diagrams

3D data : cutlines, cutplanes, iso-surfaces, iso-volumes – arrow plots, particle tracing, animations.

- Systematic data analysis by means of statistical tools.

# CHAPTER-2

# LITERATURE REVIEW

Flow field of abrupt axi-symmetric expansion is a complex phenomenon characterized by flow separation, flow recirculation and reattachment. A shear layer into two main regions may divide such a flow field, one being the flow recirculation region and the other the main flow region. The point at which the dividing streamline strikes the wall is called the reattachment point.

There is large amount of data about sudden expansion problems in literature. However, they are for specific cases of flow and geometrical parameters. Nusselt appears to have been one of the first to conduct experiments with high velocity gas flow through ducts with sudden increase in flow cross-section. From his intensive experimental study in subsonic and supersonic flow, he concluded that the base pressure will be equal to the entrance pressure if the entrance velocity is subsonic, but if the entrance flow is supersonic, the base pressure could be equal to or less than or greater than the entrance pressure.

***S. A. Khan and E. Rathakrishnan 2006*** presented an experimental investigation to study the effectiveness of micro jets to control base pressure in suddenly expanded axisymmetric ducts. Four micro jets of 1-mm orifice diameter located at 90° intervals along a pitch circle diameter of 1.3 times the nozzle exit diameter in the base region are employed as active controls. The Mach numbers at the entry to the suddenly expanded duct studied in the present study are 1.25, 1.30, 1.48, 1.60, 1.80, 2.00, 2.50 and 3.00. The jets are expanded suddenly into an axisymmetric tube with cross-sectional area 3.24 times that of nozzle exit area. The L/D ratio of the sudden expansion tube is varied from 10 to 1. As high as 40% increase in base pressure is achieved. It is found that the micro jets can serve as active controllers for base pressure. Also, the micro jets do not adversely influence the wall pressure distribution.

***Maughal Ahmed Ali Baig, et. al 2012*** studied airflow from convergent-divergent axisymmetric nozzles expanded suddenly into circular duct of larger cross-sectional area than that of nozzle exit area experimentally, focusing attention on the base pressure and the flow development in the enlarged duct. Micro-jets of 1 mm orifice diameter located at 900

intervals along a pitch circle diameter (pcd) 1.3 times the nozzle exit diameter were employed as the controller of the base pressure. The tests are conducted for Mach numbers 1.87, 2.2 and 2.58. The area ratio of the present study is 4.84. The length-to diameter ratio of the suddenly expanded duct is varied from 10 to 1 and nozzle pressure ratio (NPR) in the range 3 to 11. It is found that the active control in the form of blowing through small orifices (micro jets) are effective in controlling the base pressure field and even do not augment the flow field in the duct. An increase of 45 percent in base pressure was achieved for certain combination of parameters of the present study.

***Baoyu Guo, et. al 2002*** worked on three-dimensional, time-dependent calculations using the finite volume CFD code CFX4 and the VLES approach with standard k-e model to simulate the turbulent swirl flow in an axisymmetric sudden expansion with an expansion ratio of 5.0 for a Reynolds number of 105. This flow is unstable over the entire swirl number range considered between 0 and 0.48, and a large-scale coherent structure is 5 found to precess about the centerline. Compared with the unswirled case, inclusion of a slight inlet swirl (swirl number below 0.23) can reduce the precession speed, cause the precession to be against the mean swirl and suppress the flapping motion. Several modes of precession are predicted as the swirl intensity increases, in which the precession, as well as the spiral structure, reverses direction. Accompanying the transition between different modes, abrupt changes in precession frequency are also experienced. Grid sensitivity and comparison with smaller expansion ratio data are also discussed.

***Shafiqur Rehman and S.A. Khan 2008*** presented the results of an experimental investigation carried out to control the base pressure in a suddenly expanded axisymmetric passage. Design/methodology/approach – Four micro-jets of 1mm orifice diameter located at 908 intervals along a pitch circle diameter of 1.3 times the nozzle exit diameter in the base region was employed as active controls. The test Mach numbers were 1.25, 1.3, 1.48, 1.6, 1.8, 2.0, 2.5 and 3.0. The jets were expanded suddenly into an axi-symmetric tube with cross-sectional area 4.84 times that of nozzle exit area. The length-to-diameter ratio of the sudden expansion tube was varied from 10 to 1. Nozzles generating the above jet Mach numbers were operated with nozzle pressure ratio in the range 3-11. As high as 40 per cent increase in base pressure was achieved. In addition to base pressure, the wall pressure in the duct was also measured. They found that the wall pressure is not adversely influenced by the micro jets. The paper provides information on internal supersonic flow.

***Abbas Mansoori, et. al 2007*** found using abrupt expansion as an energy dissipater in bottom outlet of dams may have unfavorable effects on dam safety due to cavitation. Domain and intensity of cavitation, depends on magnitude and location of negative pressure. Therefore predicting the extent and intensity of negative pressure plays an important role in detection of cavitation. On the other hand, there is no globally accepted turbulence model to predict negative pressure. In this paper an experimental investigation has been performed to determine the variation of pressure. Different turbulent models were ranked through the comparison of analytical and experimental results. It was found that the Realizable k - E model has better prediction with respect to the others.

***K.M.Pandey, and Sushil Kumar 2010*** done the analysis of flow at Mach number 2.4 with fuzzy logic approach to have smooth flow in the duct. Here there are three primary pressure ratio chosen for the enlarged duct, 2.10, 2.65 and 3.48. The area ratio is taken as 2.89. The study is analyzed for length to diameter ratio of 1.24 and 6. The nozzle used is a conical one with Mach number 2.4 at exit. The analysis based on fuzzy logic theory indicates that the length to diameter ratio of 4 is sufficient for smooth flow development keeping in view all the three parameters like base pressure, wall static pressure and total pressure loss.

***R. Jagannath, et. al 2007*** studied pressure loss in suddenly expanded ducts is with the help of fuzzy logic as a tool. It is observed that minimum pressure loss takes place when the length to diameter ratio is one and it is seen that the results given by fuzzy logic formulation are very logical and it can be used for qualitative analysis of fluid flow in flow through nozzles in sudden expansion.

***Sher Afghan Khan and E. Rathakrishnan 2002*** An experimental investigation was carried out to study the effectiveness of micro-jets to control base pressure in suddenly expanded axi-symmetric ducts. Four micro-jets of 1 mm orifice diameter located at 900 intervals along a pitch circle diameter of 1.3 times the nozzle exit diameter in the base region were employed as active controls. The Mach numbers of the suddenly expanded flows were studied 2.0, 2.5 and 3.0. The jets were expanded suddenly into an axi-symmetric tube with cross-sectional area 2.56, 3.24, 4.84, and 6.25 times that of nozzle exit area. The length-to-diameter ratio of the sudden expansion tube was varied from 10 to 1. The jets were operated at an overexpansion level of (Pe/Po =) 0.277. The wall pressure

distribution in the suddenly enlarged duct was also measured. It is found that the micro-jets can serve as active controllers for base pressure. Also, the wall pressure distribution is not adversely influenced by the micro-jets. From the present investigation it is evident that for a given Mach number and nozzle pressure ratio

# CHAPTER 3

# DESIGN AND MODELLING

## 3.1 DESIGN SETUP

The geometry specification is important in any kind of CFD simulation. It is fascinating to report the physical boundaries that contain the fluid as accurately as possible, particularly for engineering issues, wherever sometimes the impact of one or more synthetic, or design, objects are to be predicted. Any inaccurate specification of the boundary surfaces may give erroneous result. Geometric setup and grid generation used to take a month or longer to perform. Presently, the geometry setup and grid generation processes have been made effortless, since almost all the packages have CAD systems and automatic grid generation segments.

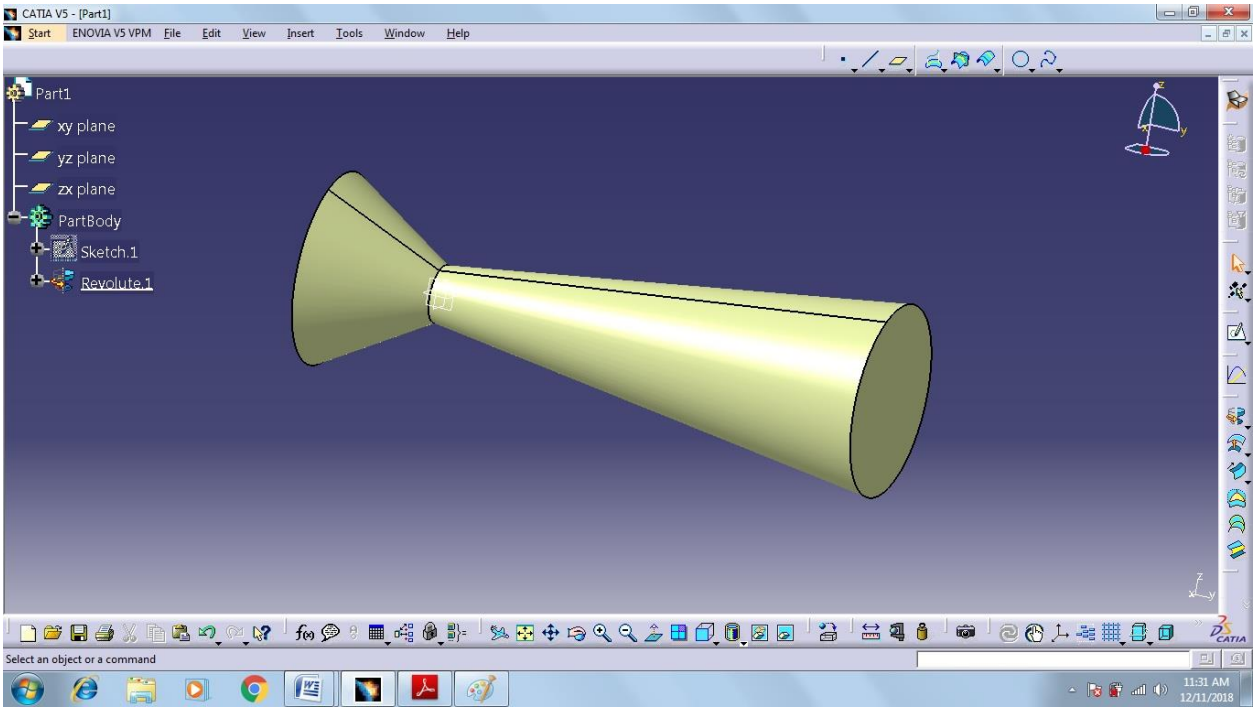


**Fig 3.1: Schematic of Supersonic Nozzle**

**Table 3.1: INPUT AND OUTPUT BOUNDARY CONDITIONS**

| No | **Input** | value |
|---|---|---|
| 1. | Input width | 1.00(m) |
| 2. | Throat width | .304(m) |
| 3. | Exit width | .861(m) |
| 4. | Throat radius curvature | .228(m) |
| 5. | Convergent length | 2.5(m) |
| 6. | Divergent angle | 5,10,15(degs) |
| 7. | Convergent angle | 30 (deg) |
| 8. | Total pressure | 45(bar) |
| 9. | Total temperature | 3400(k) |
| 10. | Mass flow rate | 826kg/s |

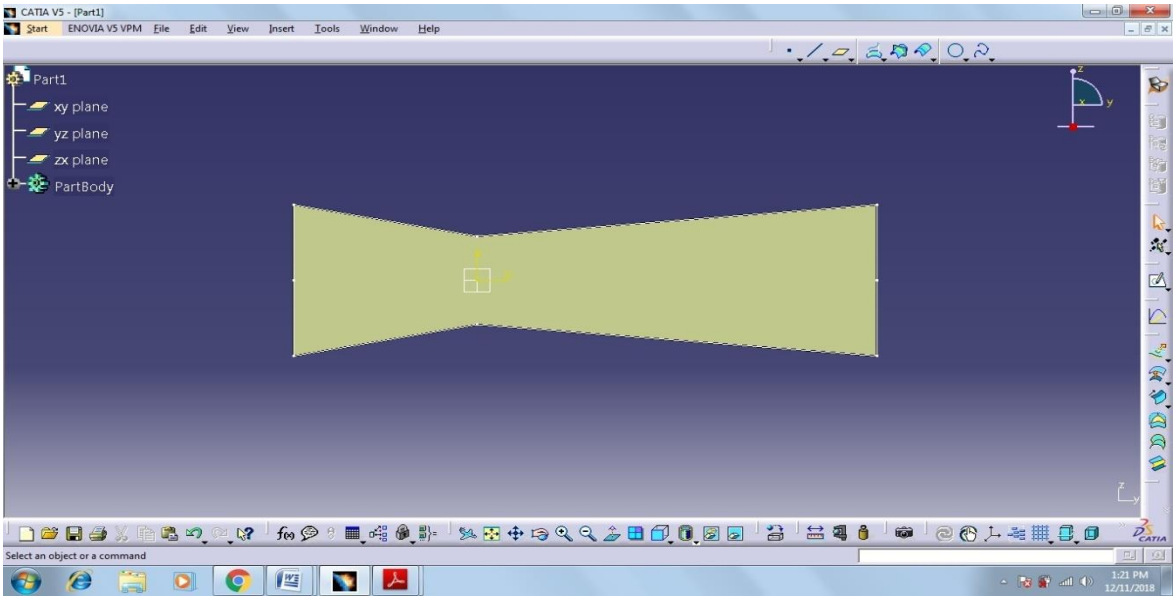


**Fig 3.2: Supersonic Nozzle at 5 deg divergent angle**

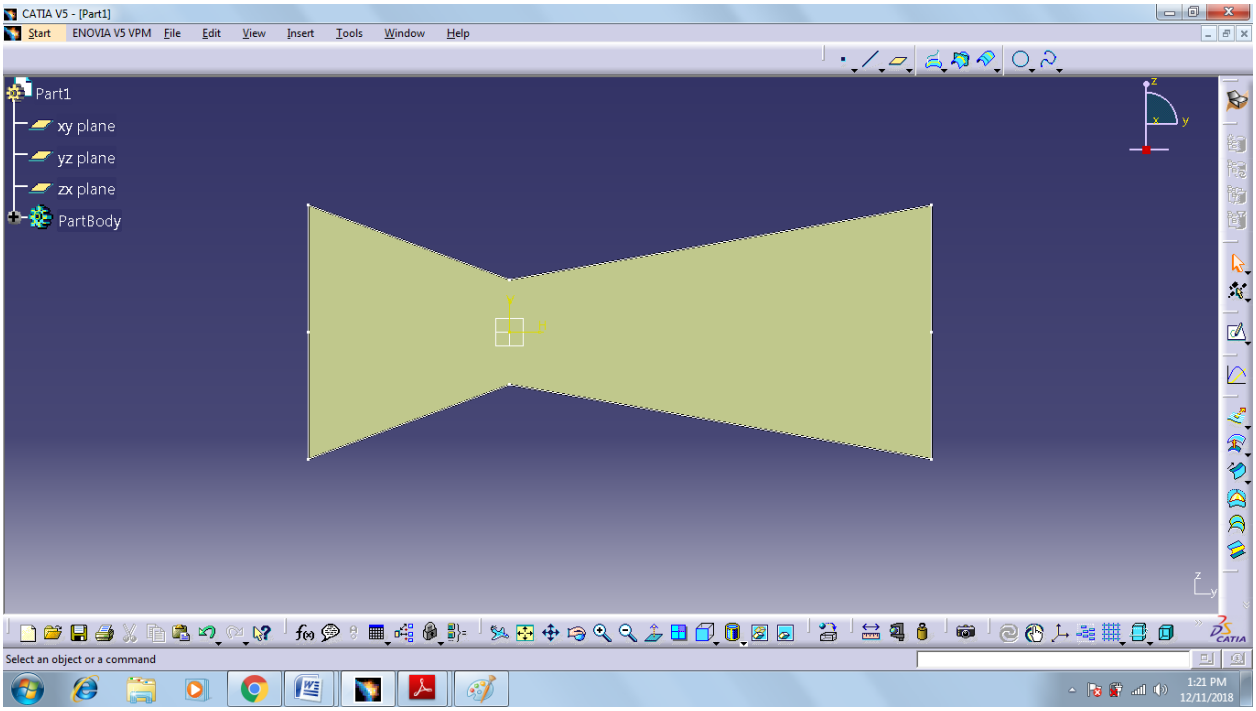


**Fig 3.3: Supersonic Nozzle at 10 deg divergent angle**

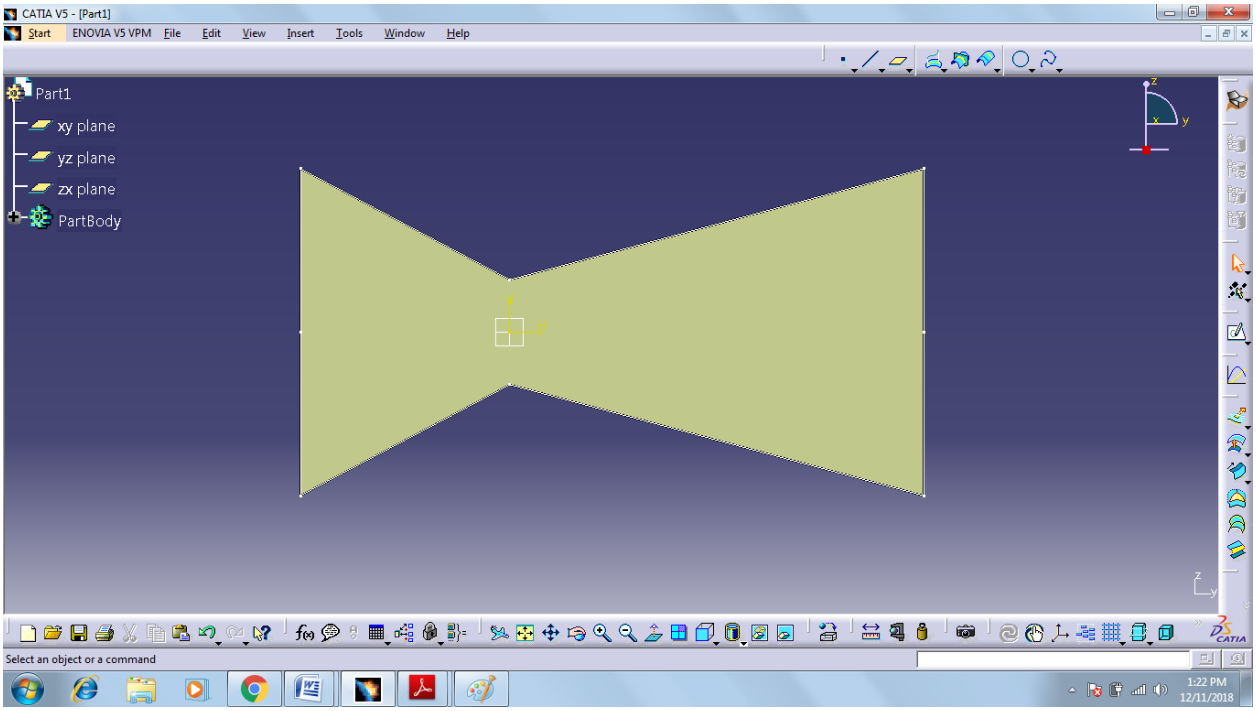


**Fig 3.4: Supersonic Nozzle at 15 deg divergent angle**

# CHAPTER 4

# RESULTS AND DISCUSSION

**Velocity magnitude at divergent angle of 5°**

It can be infer from velocity contour of the nozzle that the divergent angle of 5° shows the formation of oblique shock in the divergent section. As it is infer in Figure 4.3, across the shock, the velocity suddenly drops from 1.38e+03 m/s to 1.18e+03 m/s. After this the velocity of flow again increases. The positions where the shock occurs can be determined from the Velocity magnitude Vs position plot.

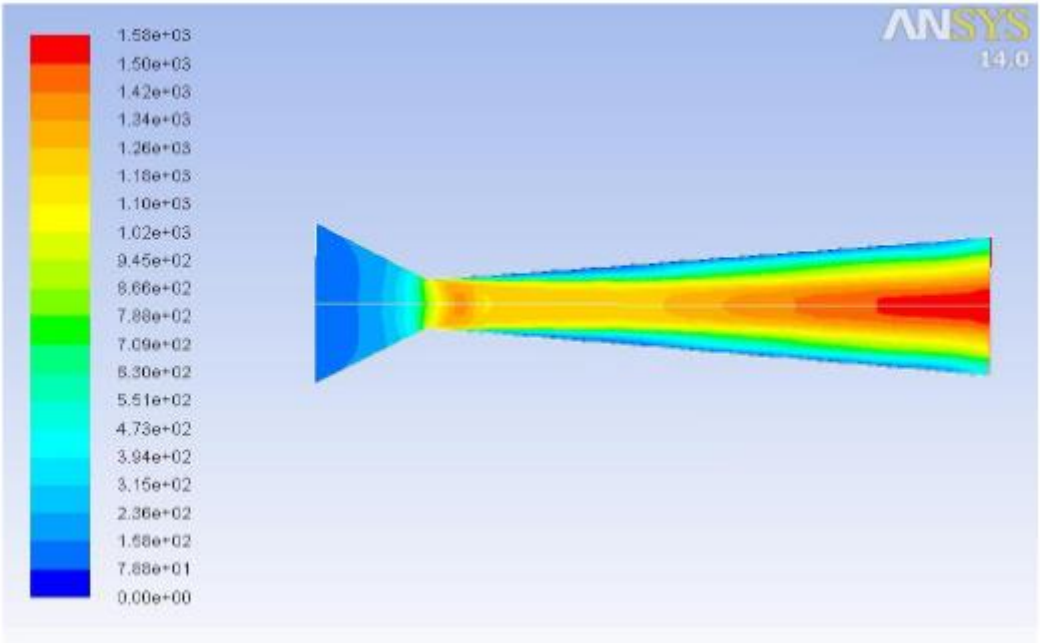


**Fig 4.1: Contour of velocity (Mach no.) at divergent angle of 5°**

You can easily visualize effect of viscous near the wall of nozzle which resulted in to lower velocity region depicted by string of blue shade. It is found that shock occurs at the position 0.25m from the throat section. The velocity magnitude is found to increase as we move from inlet to exit. The velocity at the inlet is 0.98e+02 m/s (sub-sonic). At the throat section the velocity varies from 4.32e+02 m/s to 1.35e+03 m/s. The velocity at the exit was found to be 1.592e+03 m/s (super-sonic). From this plot it is clearly observed that the velocity is increased as goes from inlet to outlet section of nozzle.

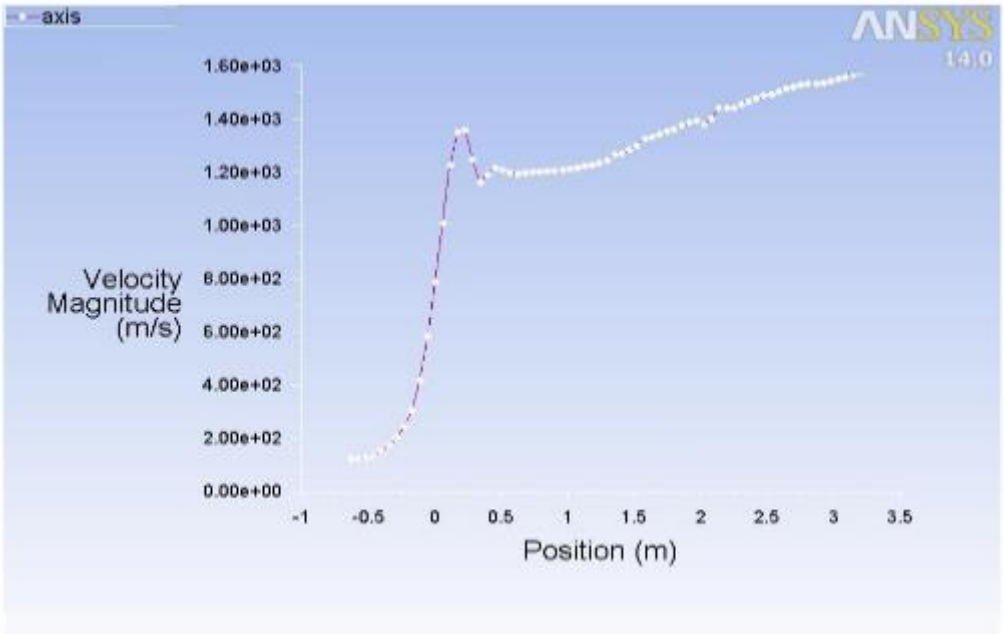


**Fig 4.2: Velocity magnitude Vs Position plot at 5° of divergent angle**

**Static Pressure at divergent angle of 5°**

Static pressure is the pressure that is exerted by a fluid. Specifically, it is the pressure measured when the fluid is still, or at rest. Contours of static pressure in convergent, throat, divergent and exit section is shown. The below figure reveals the fact that the gas gets expanded in the nozzle exit. The static pressure in the inlet is observed to be 8.52 e+06 Pa and as we move towards the throat there is a decrease and the value at the throat is found out to be 5.88e+06 Pa. After the throat, there is a sudden increase in the static pressure at the axis which indicates the occurrence of the shock. Then it reduces to a value of 1.36e+05 Pa at the exit section due to the expansion of the fluid towards the exit of the nozzle. As we can see that, maximum static pressure was noted at combustion chamber.

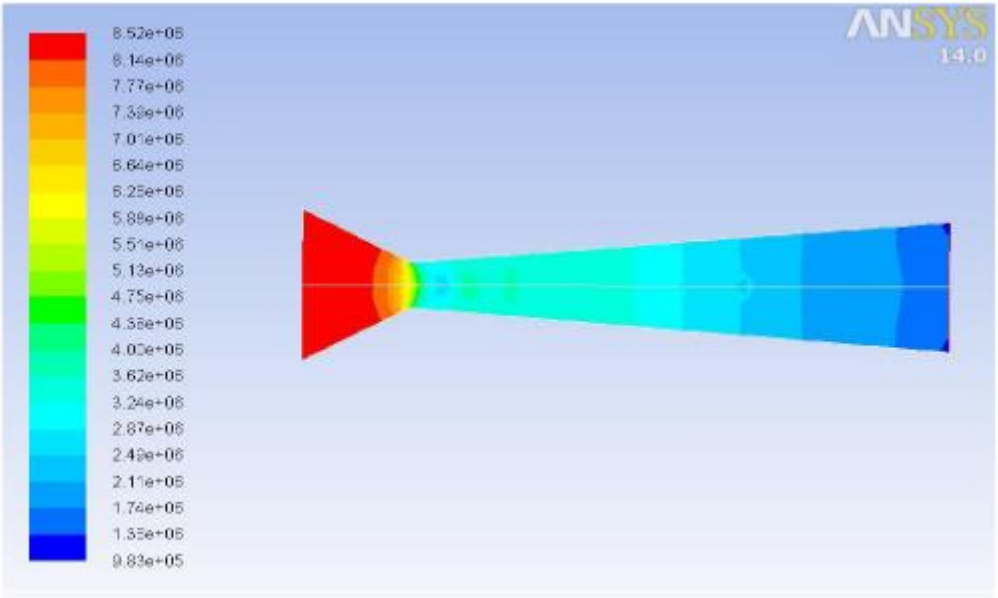


**Fig 4.3: Contour of static pressure at divergent angle of 5°**

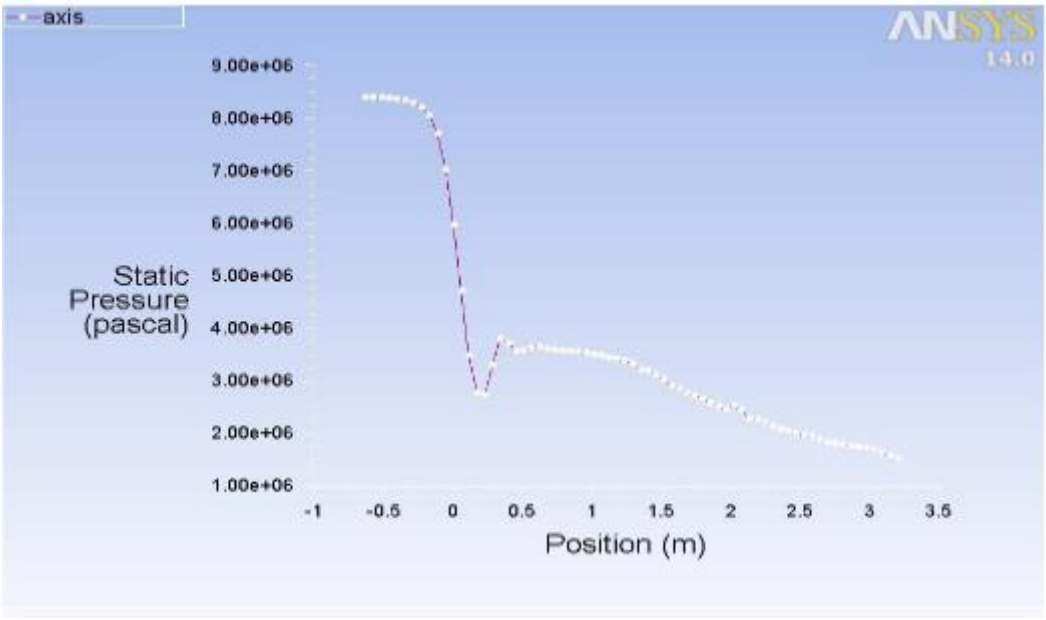


**Fig 4.4: Static Pressure VS Position plot at 5° of divergent angle**

**Static Temperature at divergent angle of 5°**

The temperature almost remains a constant from the inlet up to the throat after which it tends to decrease. At the inlet and the throat the temperature is 3.32e+03 K. After the throat, the temperature decreases till the exit. As we move from the centre vertically upwards and downward temperature increased. As we have assumed the combustion property of fluid, the static pressure is directly proportional to the static temperature. The static temperature decrease corresponding to decrease in static pressure. There is formation of shock hence static temperature increase due to decrease mach number across the shock.

Static temperature is higher in combustion chamber compared to throat and divergent.

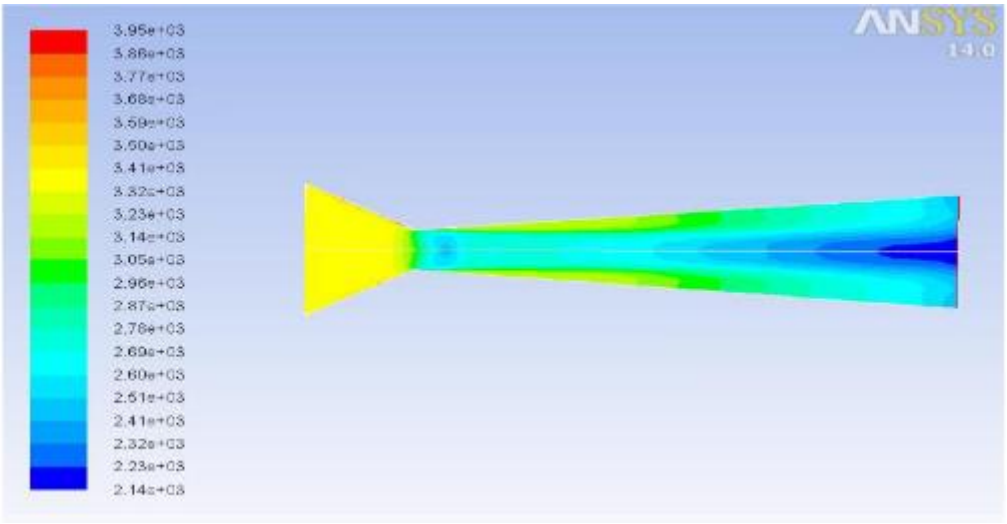


**Fig 4.5: Contour of Static Temperature at 5° of divergent angle**

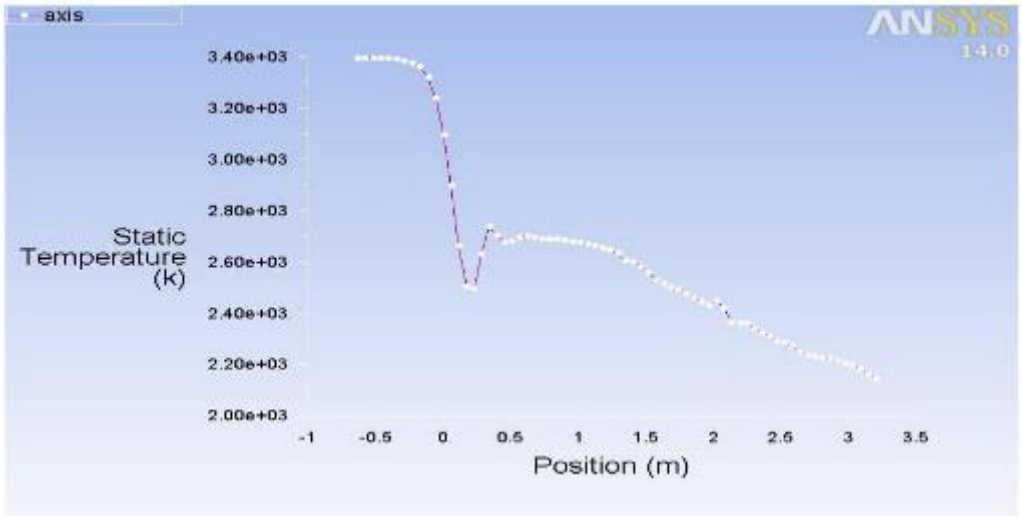


**Fig 4.6: Static Temperature Vs Position plot at 5° of divergent angle**

**Turbulent intensity at divergent angle of 5°**

The turbulent intensity contour shows that the inlet section has very low turbulence of the value 1.01e+00% and it increases towards the nozzle. Just as the divergent section starts the contour show very high value of turbulent intensity which is due to the sudden expansion of the flow into the divergent section. Here in this case the flow in the divergent section is highly turbulent because of the formation of two shocks inside the section. From the contour the region of shock has a turbulence intensity of 2.24e+01% and then it drops to 1.56e+01% at the exit section.

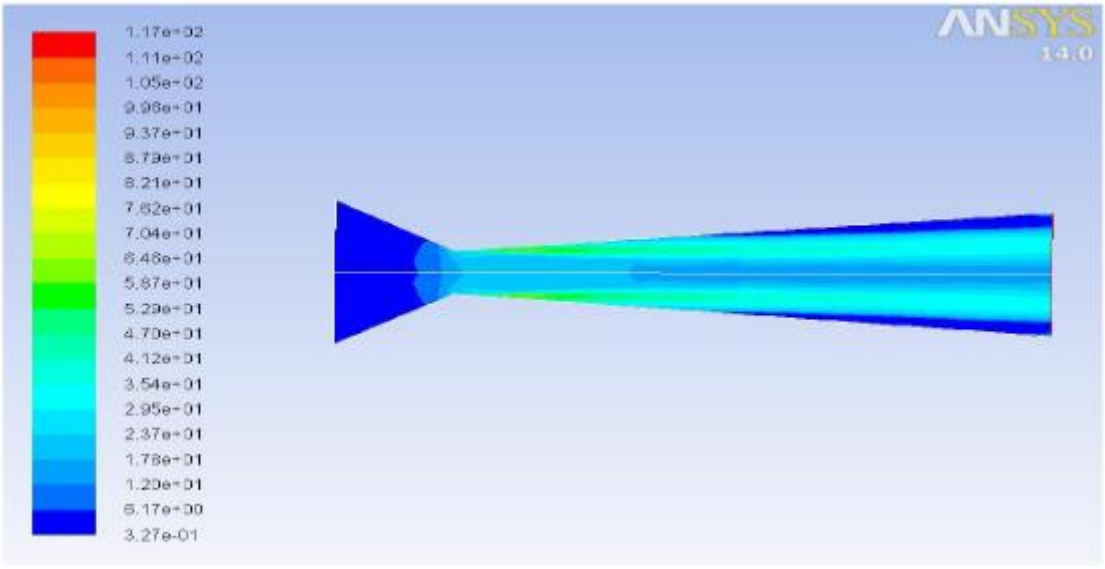


**Fig 4.7: Contour of turbulent intensity at divergent angle of 5°**

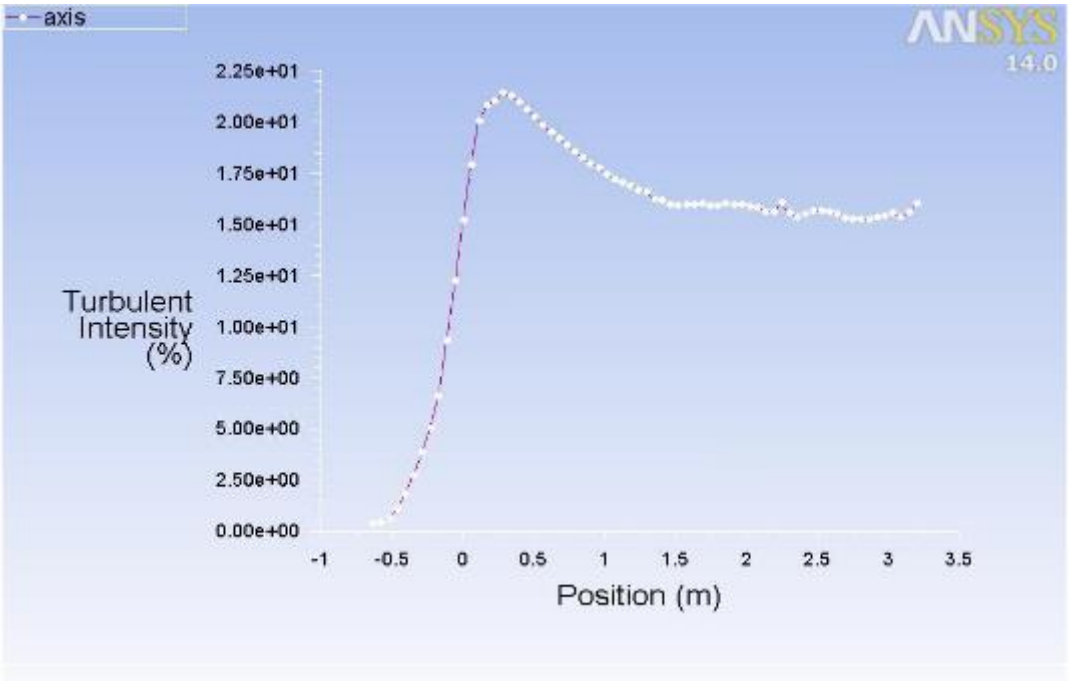


**Fig 4.8: Turbulent intensity VS Position plot at 5° of divergent angle**

**Velocity magnitude at divergent angle of 15°**

The contour of velocity magnitude of convergent-divergent nozzle when the divergent angle is made 15° is shown in the figure 10. It is clear that the shock has been completely eliminated from the divergent section of the nozzle. The inlet section has a velocity of 1.11e+03 m/s and it increases to a value of 3.61e+01m/s at the throat section. The velocity is found to be increasing as it passes through the divergent section. At the exit section, the velocity is found to be 5.28e+03 m/s. Parallel flow is observed which is a

characteristic of the conical nozzle and its design purpose (for supersonic speed) is also solved. Velocity magnitude near the wall is less due to the viscosity and the turbulence. The velocity magnitude for the default 5 degrees angle turns out to be 1.592e+02 m/s but for a divergence angle of 20 degrees it comes out to be 5.28e+03 m/s. This is due to the change in the geometry hence flow pattern also change.

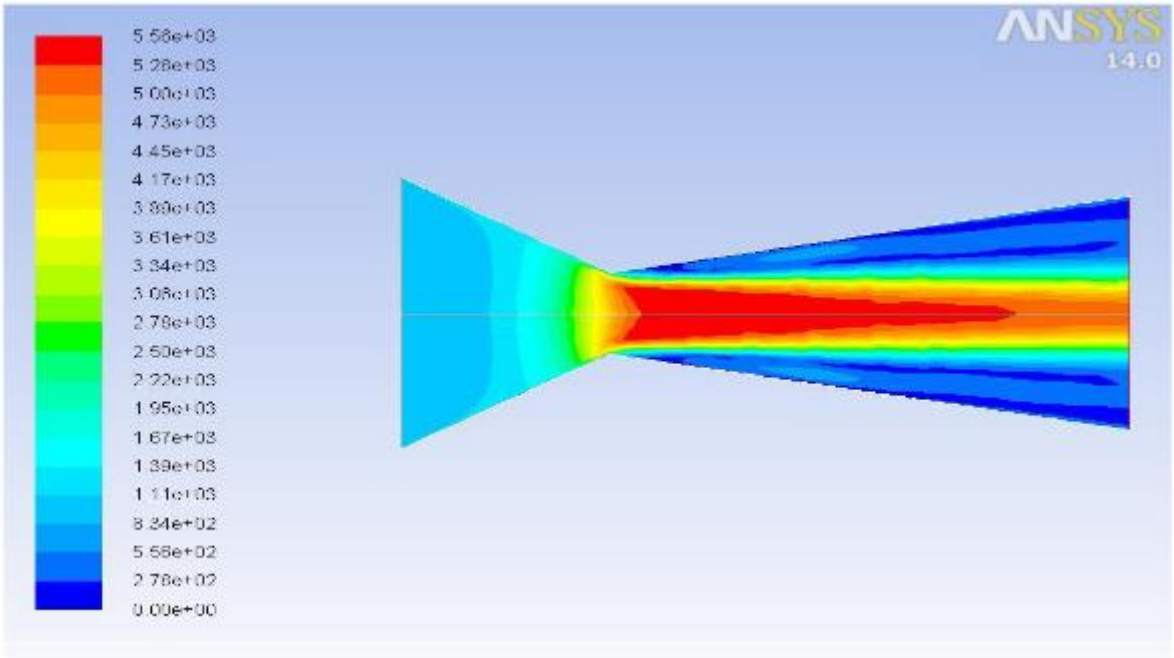


**Fig 4.9: Contour of Velocity magnitude at divergent angle of 15°**

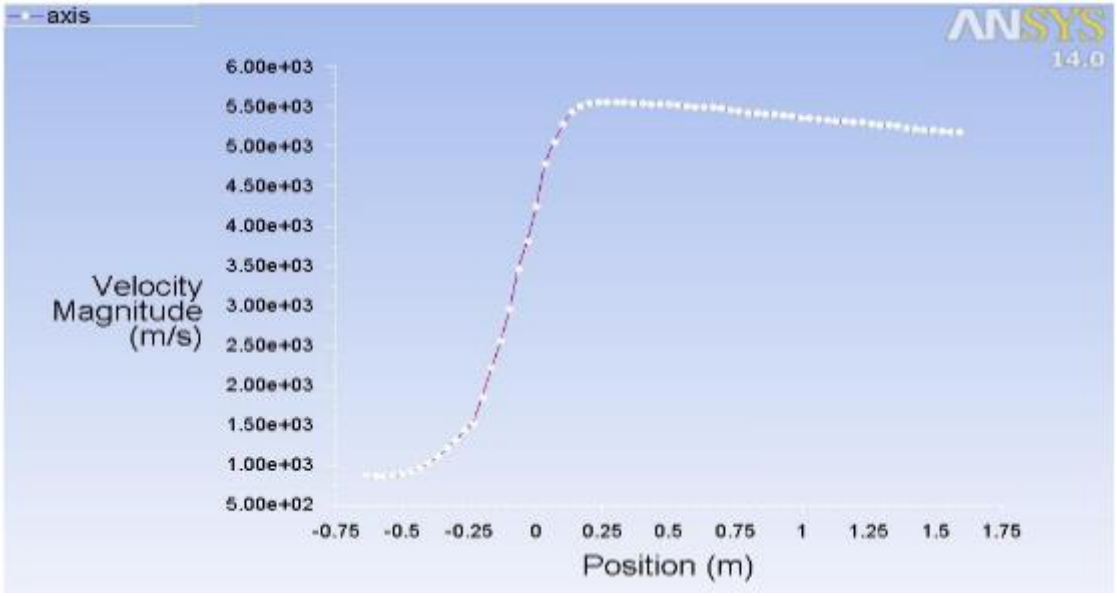


**Fig 4.10: Velocity magnitude VS Position plot at 15° divergent angle**

**Static Pressure at divergent angle of 15°**

The below Figure 12, shows that the gas gets over expanded in the nozzle exit and oblique shock is prevented. The static pressure in the inlet is observed to be 1.80e+07 Pa and the value at the throat is found out to be 5.40e+06 Pa. At the exit the pressure is experienced to be 1.25e+05 Pa. Right from the inlet to the throat to the exit the static pressure tends to decrease and remains constant till exit section. There is a considerable decrease observed after the throat to the exit where there is a large drop in the static pressure. As compared to the previous case of divergent angle of 15 degree there is a change in the exit static pressure value because of change in geometry of nozzle. This reduction in pressure intensity is directly proportional to increment in kinetic energy in form of thrust gained from nozzle at outlet section, an essential property for successful launching of rocket.

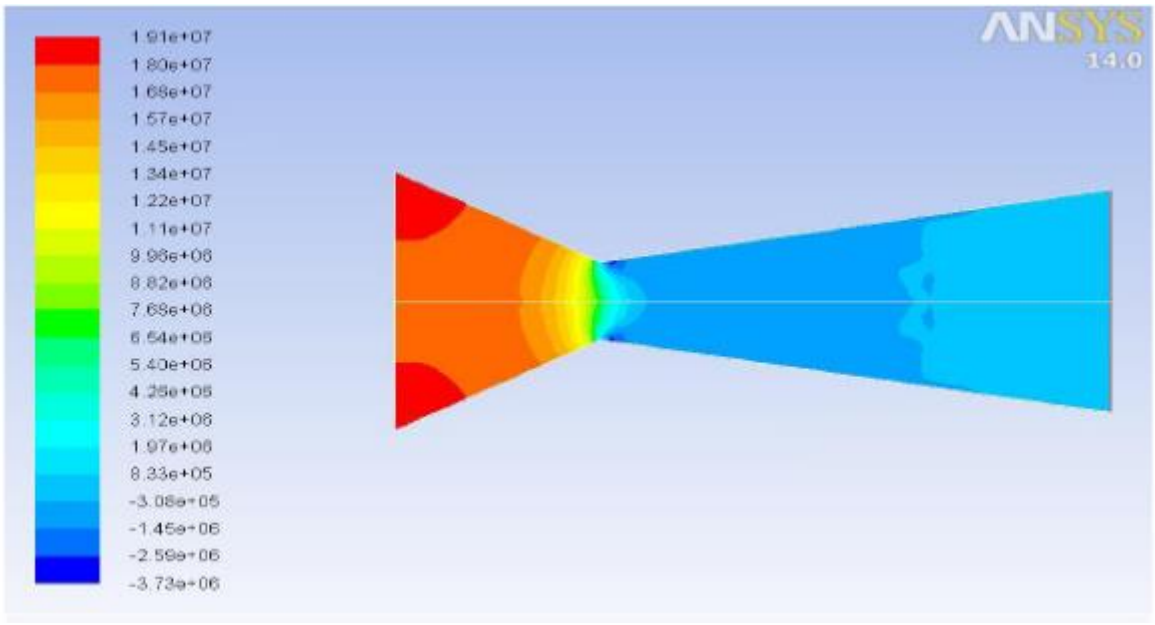


**Fig 4.11: Contour of Static Pressure at divergent angle of 15°**

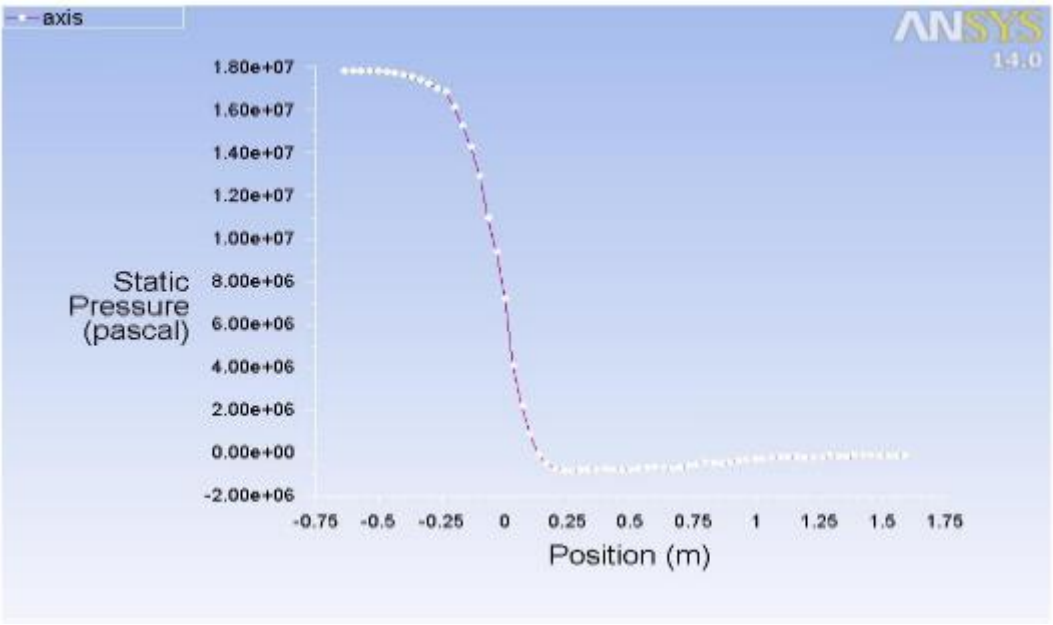


**Fig 4.12: Static Pressure VS Position plot at 15° of divergent angle**

**Static Temperature at divergent angle of 15°**

The static temperature almost remains a constant in the inlet up to the throat. Increase is observed after some distance from the throat towards the exit. Near the walls the temperature decreases to 2.65e+03 K. In the inlet and the throat the temperature is 3.32e+03 K. After the throat, the temperature increases to 4.06e+03 K at the exit. At the exit, moving vertically upward there is variation. The maximum value is not attained at the centre but at some distance from the centre. At the centre it is 3.59e+03 K and at the wall it is 2.65e+03 K. The maximum value of 4.06e+03 K is attained near the walls but some distance away from it. As pressure energy of combustion gases convert in to high kinetic energy in order to generate thrust, this increment in kinetic energy also increase collision between molecules and static temperature goes up, while total temperature remains constant. The fact that in the default nozzle with 5 degrees of divergent angle, the temperature increases as soon as the throat is crossed but in this it is clearly observed that there is a beginning in the rise in temperature after some distance from the throat.

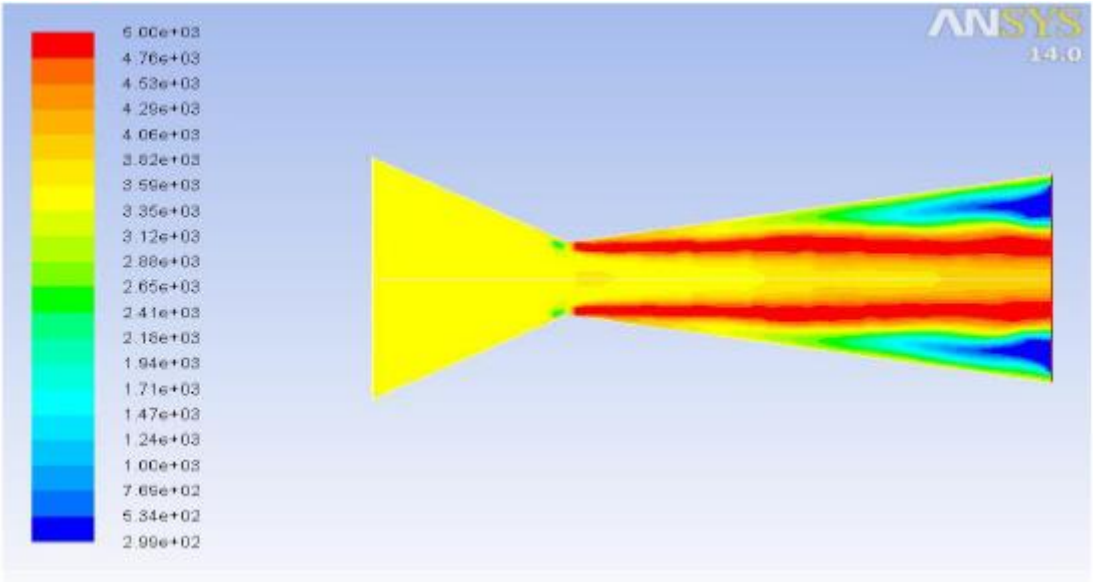


**Fig 4.13: Contour of Static Temperature at divergent angle of 15°**

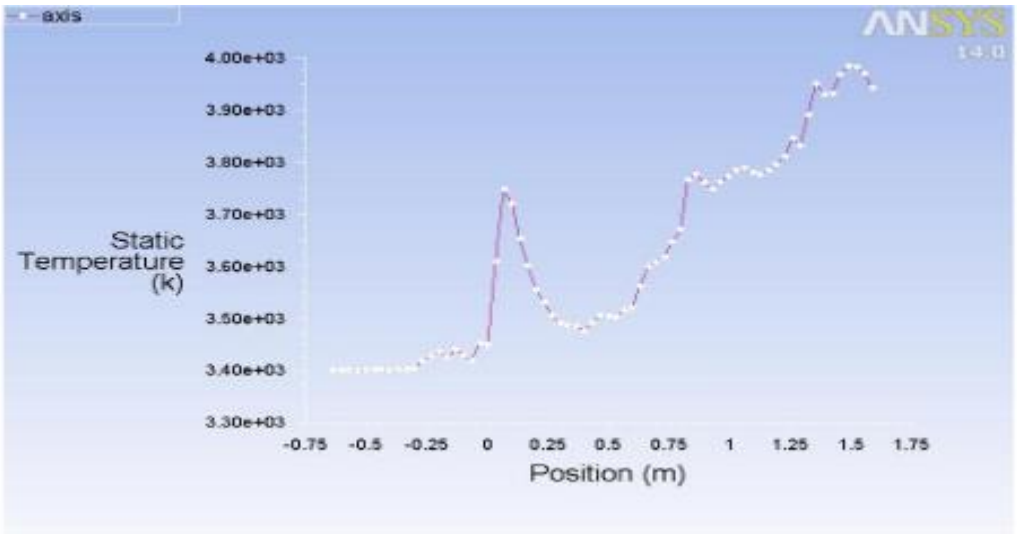


**Fig 4.14: Static Temperature VS Position plot at 15° divergent angle**

**Turbulent intensity at divergent angle of 15°**

The turbulent intensity contour shows that at the inlet the turbulent intensity is 1.01e+00%. It has increased to 2.40e+01% at the throat section. Since the divergent angle is higher, the sudden expansion has caused the turbulence at the beginning of the divergent section. It is also seen that the increasing velocity towards the exit section also has caused a turbulence of flow towards the exit section. The value of turbulence is found to be 2.25e+01% in this region.

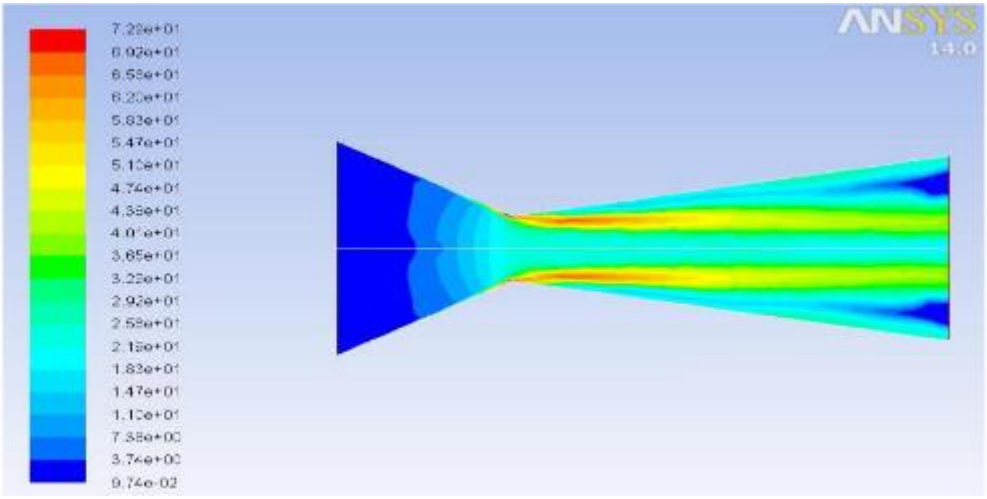


**Fig 4.15: Turbulent intensity VS Position plot at 15° divergent angle**

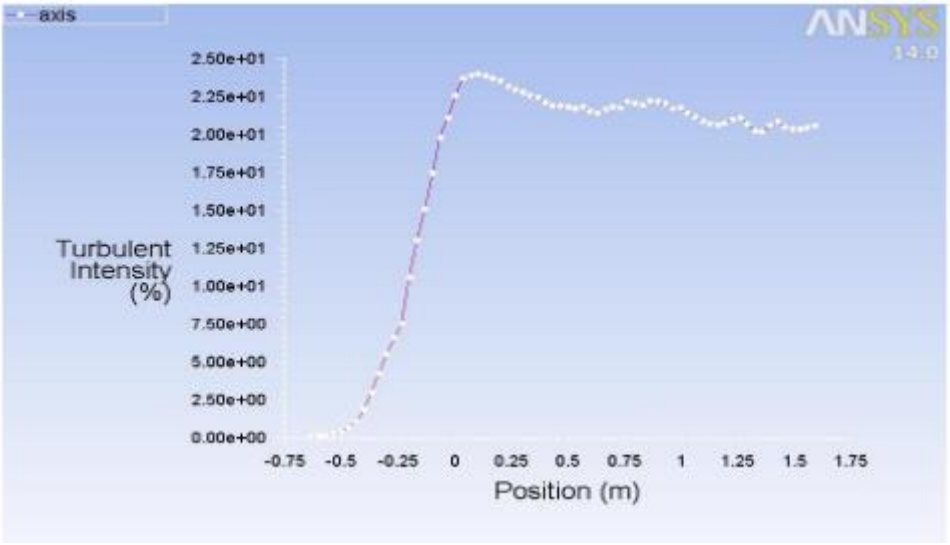


**Fig 4.16: Turbulent intensity Vs Position plot at 15° divergent angle**

## CONCLUSIONS

In this project we studied the performance and efficiency of supersonic nozzle under different divergent angle i.e. (5, 10, 15 deg) by using two dimensional axis-symmetric model, which solves governing equation by a control volume method. Variation in parameters like velocity, static pressure, turbulence intensity and temperature are being analyzed and model was done in Catia v5r20.

The phenomena of oblique shock are visualized and it was found that at which degree of divergent angle it is completely eliminated from nozzle. Objective of this research is to investigate best suited divergent angle.

## REFERENCES


1. H.K.Versteeg and W.Malala Sekhara, “An Introduction to Computational Fluid Dynamics”, British Library cataloguing pub, 4th edition, 1996.

2. Lars Davidson, “An Introduction to Turbulence Models”, Department of thermo and fluid dynamics, Chalmers University of Technology, Goteborg, Sweden, November, 2003.

3. Karna s. Patel, "CFD analysis of an aerofoil", International Journal of Engineering Research.

4. K.M. Pandey, Member IACSIT and A.P. Singh "CFD Analysis of Conical Nozzle for Mach 3 at Various Angles of Divergence with Fluent Software

5. Varun, R.; Sundararajan,T.; Usha,R.; Srinivasan,k.; Interaction between particle-laden under expanded twin supersonic jets, Proceedings of the Institution of Mechanical Engineers, Part G: Journal of Aerospace Engineering 2010 224: 1005.

6. Pandey,K.M.; Singh, A.P.; CFD Analysis of Conical Nozzle for Mach 3 at Various Angles of Divergence with Fluent Software, International Journal of Chemical Engineering and Applications, Vol. 1, No. 2, August 2010, ISSN: 2010-0221.

7. Natta, Pardhasaradhi.; Kumar, V.Ranjith.; Rao, Dr. Y.V. Hanumantha.; Flow Analysis of Rocket Nozzle Using Computational Fluid Dynamics (CFD), International Journal of Engineering Research and Applications (IJERA), ISSN: 2248-9622,Vol. 2, Issue 5, September- October 2012, pp.1226-1235.

8. K.M. Pandey, Member IACSIT and A.P. Singh. K.M.Pandey, Member, IACSIT and S.K.YadavK.M.Pandey and S.K.Yadav, ―CFD Analysis of a Rocket Nozzle with Two Inlets at Mach2.1, Journal of Environmental Research and Development, Vol 5, No 2, 2010, pp-308-321.

9. Shigeru Aso, ArifNur Hakim, Shingo Miyamoto, Kei Inoue and Yasuhiro Tani " Fundamental study of supersonic combustion in pure air flow with use of shock tunnel" Department of Aeronautics and Astronautics, Kyushu University, Japan , Acta Astronautica 57 (2005) 384 – 389.

10. P. Padmanathan, Dr. S. Vaidyanathan, Computational Analysis of Shockwave in Convergent Divergent Nozzle, International Journal of Engineering Research and Applications (IJERA), ISSN: 2248-9622 ,Vol. 2, Issue 2,Mar-Apr 2012, pp.1597-1605.

11. A damson, T.C., Jr., and Nicholls. J.A., "On the structure of jets from highly under expanded Nozzles into Still Air," Journal of the Aerospace Sciences, Vol.26, No.1, Jan 1959, pp. 16-24.

**12.** Lewis, C. H., Jr., and Carlson, D. J., “Normal Shock Location in under expanded Gas and Gas particle Jets,” AIAA Journal, Vol 2, No.4, April 1964, pp. 776-777.